



**T.R.
ONDOKUZ MAYIS UNIVERSITY
INSTITUTE OF GRADUATE STUDIES
DEPARTMENT OF NANOSCIENCE AND NANOTECHNOLOGY**

**REMOVAL OF LEAD, CADMIUM AND DYE BY IRON
NANOPARTICLES SYNTHESIZED BY ACTINOBACTERIA**

Master Thesis

Ali Saleh Mohammed MOHAMMED

Supervisor

Assoc. Prof. Dr. Hilal AY

SAMSUN

2022

T.R.
ONDOKUZ MAYIS UNIVERSITY
INSTITUTE OF GRADUATE STUDIES
DEPARTMENT OF NANOSCIENCE AND NANOTECHNOLOGY



**REMOVAL OF LEAD, CADMIUM AND DYE BY IRON
NANOPARTICLES SYNTHESIZED BY ACTINOBACTERIA**

Master Thesis

Ali Saleh Mohammed MOHAMMED

Supervisor

Assoc. Prof. Dr. Hilal AY

This study was funded by Ondokuz Mayıs University under project number
PYO.FEN.1904.20.005.

SAMSUN

2022

ACCEPTANCE AND APPROVAL OF THE THESIS

The study entitled “**Removal of Lead, Cadmium and Dye by Iron Nanoparticles Synthesized by Actinobacteria**” prepared by **Ali SALIH** and supervised by **Assoc. Prof. Dr. Hilal AY** was found successful and unanimously accepted by committee members as Master thesis of the Department of Nanoscience and Nanotechnology, following the examination on the date 19/01/2022.

	Title Name Surname	University	Department	Signature	Final decision
Chairman	Prof. Dr. Ekrem ATALAN	İnönü University	Department of Molecular Biology and Genetics		<input checked="" type="checkbox"/> Accept
					<input type="checkbox"/> Reject
Member	Prof. Dr. Müberra ANDAÇ	Ondokuz Mayıs University	Department of Chemistry		<input checked="" type="checkbox"/> Accept
					<input type="checkbox"/> Reject
Member	Assoc. Prof. Dr. Hilal AY	Ondokuz Mayıs University	Department of Molecular Biology and Genetics		<input checked="" type="checkbox"/> Accept
					<input type="checkbox"/> Reject

This thesis has been approved by the committee members that already stated above and determined by the Institute Executive Board.

APPROVAL

... / ... / ...

Prof. Dr. Ali BOLAT

Head of Institute of Graduate Studies

DECLARATION OF COMPLIANCE WITH SCIENTIFIC ETHIC

I hereby declare and undertake that I complied with scientific ethics and academic rules in all stages of my Master thesis, that I have referred to each quotation that I use directly or indirectly in the study and that the works I have used consist of those shown in the sources, that it was written in accordance with the institute writing guide and that the situations stated in the article 3, section 9 of the Regulation for TÜBİTAK Research and Publication Ethics Board were not violated.

İmza
2022

Ali Saleh Mohammed MOHAMMED

DECLARATION OF THE THESIS STUDY ORIGINALITY REPORT

Thesis Title: Removal of Lead, Cadmium and Dye by Iron Nanoparticles Synthesized by Actinobacteria.

As a result of the originality report taken by me from the plagiarism detection program on 01.01.2022 for the thesis titled above;

Similarity ratio : % 22

Single resource rate : % 2 has been released.

İmza
19/01/ 2022

Assoc. Prof. Dr. Hilal AY

ÖZET

AKTİNOBAKTERİLER TARAFINDAN SENTEZLENEN DEMİR NANOPARTİKÜLLERİ KULLANILARAK KURŞUN, KADMIYUM VE BOYANIN UZAKLAŞTIRILMASI

Ali Saleh Mohammed MOHAMMED
Ondokuz Mayıs Üniversitesi
Lisansüstü Eğitim Enstitüsü
Nanobilim ve Nanoteknoloji Ana Bilim Dalı
Yüksek Lisans, Ocak/2022
Danışman: Doç. Dr. Hilal AY

Nanomateriyaller, eşsiz fizikokimyasal özellikleri ve farklı alanlarda yaygın kullanımlarından dolayı yoğun ilgi çekmektedir. Metalik nanopartiküller gibi yeni nanomateriyaller, yaygın uygulama alanlarına sahiptir. Kristal veya amorf yapıdaki demir oksit nanopartikülleri, manyetik sıvılar, tanımlayıcı görüntüleme, ilaç iletimi, fiziksel ayırma, solar enerji dönüşümü, manyetik depolama ortamları, elektronik endüstrisi ve katalizörler gibi birçok alanda kullanılmaktadır. Özellikle nanometre boyutundaki amorf demir oksit nanopartikülleri geniş bir yüzey alanına sahiptir; böylece bu nanopartiküller ağır metal ve boya uzaklaştırmanın yanı sıra gaz emilimi, sensörler ve elektrot materyalleri için kullanılabilir iyi adaylardır. Bu çalışmada, demir nanopartiküllerinin sentezi için çevre dostu bir yöntem kullanılarak sentezlenen nanopartiküllerin sulu çözeltilerden kurşun, kadmiyum ve asit kırmızısı 337 boya maddesini uzaklaştırabilme etkinliği analiz edildi. Demir nanopartiküllerinin sentezi için toprak örneklerinden izole edilen yeni aktinobakteri suşları kullanıldı. Aktinobakteriler, farklı uygulama alanlarına sahip çeşitli sekonder metabolitleri sentezleme yeteneğine sahip olduğu bilinen bir mikroorganizma grubudur. Demir nanopartikülü sentezi için *Crossiella*, *Nocardia*, *Saccharothrix*, *Saccharomonospora* ve *Streptomyces* cinslerine ait toplan altı izolat kullanılmıştır. *Streptomyces* sp. SP618 izolatı tarafından sentezlenen demir nanopartiküllerinin fizikokimyasal özellikleri XRD, SEM-EDS ve FT-IR ile analiz edildi. Nanopartiküller, sulu çözeltideki (pH 3) asit kırmızısı 337 boyasını etkili bir biçimde uzaklaştırırken, bu nanopartiküllerin kurşun veya kadmiyumun uzaklaştırılmasında dikkate değer bir etkinliğinin olmadığı görülmüştür. Ayrıca, 16S rRNA gen dizi analizine dayalı olarak gerçekleştirilen filogenetik analiz, bu çalışmada nanopartikül sentezi için kullanılan izolatların ilişkili oldukları cinsler için yeni türleri temsil edebileceğini göstermektedir. Sonuç olarak bu çalışma, aktinobakteriler tarafından sentezlenen demir nanopartiküllerinin, özellikle arıtma süreçleri gibi endüstriyel uygulamalar için yüksek bir potansiyele sahip olduğunu göstermektedir.

Anahtar Sözcükler: Aktinobakteriler, 16S rRNA-temelli Filogeni, Biyolojik Sentez, Demir Nanopartikülleri

ABSTRACT

REMOVAL OF LEAD, CADMIUM AND DYE BY IRON NANOPARTICLES SYNTHESIZED BY ACTINOBACTERIA

Ali Saleh Mohammed MOHAMMED

Ondokuz Mayıs University

Institute of Graduate Studies

Department of Nanoscience and Nanotechnology

Master, January/2022

Supervisor: Assoc. Prof. Dr. Hilal AY

Nanomaterials have gained remarkable attention due to its unique physicochemical properties and extensive usage in diverse fields. Novel nanomaterials such as metallic nanoparticles may have broad application areas. Iron oxide nanoparticles in the crystalline or amorphous state have been used in many applications such as magnetic fluids, diagnostic imaging, drug delivery, physical separation, solar energy transformation, magnetic storage media, electronics industry, and catalysts. In particular, nanometre-sized amorphous iron oxide particles have a large surface area; therefore, they are good candidates for gas sorption, sensors, and electrode materials, as well as for heavy metal and dye removal. In this study, an eco-friendly approach was employed to synthesize iron nanoparticles, and their effectiveness in removing lead, cadmium, and acid red 337 from aqueous solutions was analyzed. For the synthesis of iron nanoparticles, novel actinobacterial strains isolated from soil samples were used. Actinobacteria is a group of microorganisms well-known for their capability to synthesize various secondary metabolites with different applications. A total of six actinobacteria belonging to the genera *Crossiella*, *Nocardia*, *Saccharothrix*, *Saccharomonospora* and *Streptomyces* were isolated and used for iron nanoparticle synthesis. Physicochemical characteristics of the iron nanoparticle synthesized by *Streptomyces* sp. SP618 strain were revealed by XRD, SEM-EDS and FT-IR analyses. These iron nanoparticles effectively removed acid red 337 dye from aqueous solutions at pH 3 while the nanoparticles had no considerable effect on the removal of lead or cadmium. Moreover, the phylogenetic analysis based on 16S rRNA gene sequences revealed that the isolates revealed by this study might represent novel species within their corresponding genera. In conclusion, this study showed that iron nanoparticles synthesized by actinobacteria have a high potential for industrial applications, particularly for remediation processes.

Keywords: *Actinobacteria*, 16S rRNA-based phylogeny, Biological Synthesis, Iron Nanoparticles.

ACKNOWLEDGEMENT

This research behind it would not have been possible without the exceptional support of my supervisor, so I would like to thank my supervisor Assoc. Prof. Dr. Hilal AY.

Ali Saleh Mohammed MOHAMMED

CONTENTS

ACCEPTANCE AND APPROVAL OF THE THESIS.....	i
ABBREVIATIONS OF TERMS	vii
FIGURES LEGENDS.....	viii
TABLES LEGENDS.....	ix
1. INTRODUCTION	1
2. NANOTECHNOLOGY	4
2.1. Applications and Benefits Of Nanotechnology.....	4
2.2. Environmental Nanotechnology.....	8
2.2.1. Application in Environment.....	8
2.3. Approaches of Synthesis of the Nano-Materials.....	9
2.4. Green Nanotechnology.....	11
2.5. Characterization of NPs.....	11
2.6. Iron nanoparticles.....	13
2.7. Biogenic Synthesis.....	17
2.8. Actinobacteria.....	17
2.9. Biological NP Synthesis by Actinobacteria.....	19
2.10. Heavy Metals.....	19
3. MATERIALS AND METHOD	22
3.1. Selective Isolation of Actinobacteria.....	22
3.2. Identification of Bacterial Isolates.....	23
3.3. Nanoparticles Synthesis.....	25
3.4. Characterizations of Iron Nanoparticles.....	25
3.4.1. UV-Vis Spectrophotometry.....	25
3.4.2. X-Ray Diffraction (XRD) Analysis.....	26
3.4.3. Scanning Electron Microscopy (SEM).....	26
3.4.4. FT-IR analysis.....	26
3.5. 3 Heavy Metal Removal Assay.....	26
3.6. Dye Removal Activity.....	26
3.6.1. Red Dye Preparation.....	27
3.6.2. Effect of pH.....	28
3.6.3. Effect of Contact Time on Adsorption.....	28
4. RESULTS AND DISCUSSION.....	29
4.1. Identification and Phylogenetic Analysis of <i>Actinobacteria</i>	29
4.2. Characterization of Iron Nanoparticles Synthesized by <i>Actinobacteria</i>	32
4.3. Heavy Metal Removal Assay.....	34
4.4. Dye Removal Activity.....	35
5. CONCLUSIONS.....	38
REFERENCES.....	39
APPENDIX I.....	44
APPENDIX II.....	44
APPENDIX III.....	44
BACKGROUND.....	53

ABBREVIATIONS OF TERMS

INP	: Iron nanoparticles
IONP	: Iron oxide nanoparticle
NP	: Nanoparticle
CNT	: carbon nanotube
Co	: initial value
Ce	: final value
SEM	: Scanning electron microscopy
XRD	: X-Ray Diffraction
FTIR	: Fourier transform infrared
TEM	: Transmission electron microscopy
UVS	: UV-Vis spectrometry

FIGURES LEGENDS

Figure 2.1. Application fields of nanotechnology	7
Figure 2.2. Two approaches for nanoparticles synthesis	11
Figure 2.3. Various methods of preparation of nanoparticles	15
Figure 2.4. Iron oxide nanoparticles.....	16
Figure 2.5. Actinobacteria isolate appearance on the Starch casein agar plate. a, c Plate view of the isolates of the Actinobacterial. b, d Morphology of the individual colonies (Anandan <i>et al</i> , 2016).....	18
Figure 3.1. Soil samples	22
Figure 3.2. Precipitated iron nanoparticles (SP 618)	25
Figure 4.1. Maximum likelihood tree for strains <i>Streptomyces</i> spp. SP618, SP654 and its close phylogenetic neighbours interpreted under the GTR+GAMMA model and rooted at the mid-point. Scale bar represents the expected number of the substitutions in each one of the sites. The support values for the bootstrapping have been shown above branches in the case of 60% for the maximal possibility (left) and maximal parsimony (right). GenBank accession numbers for 16S rRNA gene sequences have been provided between the brackets	29
Figure 4.2. Maximum likelihood tree for strain <i>Nocardia</i> sp. SN13 and its close phylogenetic neighbours that had been interpreted under GTR+GAMMA model and rooted at the mid-point. Scale bar is indicating expected number of the substitutions in each one of the sites. The support values for the bootstrapping have been illustrated the branches in the case where it is > 60% for the maximal parsimony (right) and maximal possibility (left). GenBank numbers of accession for 16-S rRNA gene sequences have been provided between the brackets (Figure 4.2).	30
Figure 4.3. Maximum likelihood tree for strain <i>Crossiella</i> sp. SN42and its close phylogenetic neighbours interpreted under GTR+GAMMA model and rooted at the mid-point. Scale bar indicates the expected amount of the substitutions in each one of the sites. Support values for the bootstrapping have been provided above branches in the case where >60% for maximal parsimony (right) and maximal possibility (left). The accession numbers of the GenBank for 16-S rRNA gene sequences have been provided between the brackets..	31
Figure 4.4. Maximum likelihood tree for strain <i>Saccharothrix</i> sp. SN43 and its close phylogenetic neighbours interpreted under GTR+GAMMA model and rooted at the mid-point. Scale bar indicates expected amount of the substitutions in each one of the sites. The bootstrapping support values have been given above branches when > 60% for maximal parsimony (right) and maximal possibility (left). The GenBank accession numbers for 16-S rRNA gene sequences have been provided between the brackets	31
Figure 4.5. Maximum likelihood tree for strain <i>Saccharomonospora</i> sp. YS38 and its close phylogenetic neighbours interpreted under the GTR+GAMMA model and rooted at the mid-point. Scale bar indicates expected amount of the substitutions in each one of the sites. The bootstrapping support values are given above branches when > 60% for maximal parsimony (right) and maximal possibility (left). The accession numbers of the GenBank for 16-S rRNA gene sequences have been provided between the brackets	32
Figure 4.6. XRD patterns of the iron nanoparticles that have been synthesized by strain SP618.....	33
Figure 4.7. SEM image of iron nanoparticles synthesized by strain SP618 at 100 nm scale resolution.....	33
Figure 4.8. EDX results of synthesized NPs possessing strong Iron signals	34
Figure 4.9. FT-IR spectra of iron oxide nanoparticles synthesized by strain SP618.....	34
Figure 4.10. Concentration effect.....	35

TABLES LEGENDS

Table 3.1. Iron nanoparticles used for dye removal assay	27
Table 4.1. Pairwise sequence identity levels of strains to the closest type species	29
Table 4.2. Result of atomic absorption spectroscopy	35
Table 4.3. Different concentration of iron nanoparticles with fix concentration of red dye ..	35
Table 4.4. Effect of time contact of adsorption	36
Table 4.5. Filter effect with time on adsorption	37
Table 4.6. Acid red 337 dye removal activity of iron nanoparticles synthesized by strain SP618.....	37

1. INTRODUCTION

Due to their uses in health, electronics, and environmental cleanup, nanoparticles (NPs) have gotten a lot of attention in the last 10 years. Scientists have been able to create valuable materials in low dimensions, like metal oxides, metals, hybrid materials, and semiconductors, thanks to advances in nanotechnology (García-Cañas *et al*, 2014). In nanomaterial research, metal NPs are one of the most common compounds. Iron (Fe) is a one-of-a-kind element which may exist in a variety of valence states, from zero to three. Furthermore, each one of the Fe compounds has different characteristics, ranging from magnetic to Ferro magnetic. Due to their distinctive capabilities and structure, Fe and its compounds, like zero-valent Fe_3O_4 and Fe_2O_3 , have piqued attention for use in drug delivery, imaging, sensors, gene delivery, and catalysis (Kouhbanani *et al*, 2019), Iron oxide NPs (IONPs) were majorly utilized in biotechnology, medical science, and environmental sciences due to their remarkable physicochemical features, increased intrinsic reactivity, and strong catalytic activities. Many effective synthesis approaches, like biosynthetic and chemical processes, were developed to date for synthesizing IONP (Zikalala *et al*, 2018). With global industrialization in the twenty-first century, the use of various pigments and dyes has become a concern to the environment. They are employed in various industries, which include cosmetics and medicine, in addition to textiles. Because of their capability to connect tightly with materials, minimal energy consumption, ease of application, and wide range of bright colors, azo dyes are one of the most commonly used dye groups in dyeing units (Kishor *et al*, 2018). NPs are more and more being utilized in environmental remediation due to their capacity for the reduction of the costs and improving the overall remediation methods' efficiency, Nano remediation is using reactive NPs for detoxification and transformation of pollutants by catalytic processes or chemical reduction. Different NPs have been successfully used for the dye degradation, like the TiO_2 , FeO, Zinc Ferrite and Manganese-doped ZnO (Mardikar *et al*, 2021).

Lately, due to the increase in the prominence of the nano-technologies, the iron oxide NPs (IONPs) had been applied in the elimination of dye contamination. IONPs in the amorphous or crystalline state were utilized in several applications, like the magnetic fluids, drug delivery, diagnostic imaging, solar energy transformations, biological separation, electronics industry, magnetic storage media, and catalysts.

Several nanoparticles, including FeO, TiO₂, Manganese-doped ZnO, and Zinc Ferrite, have been effectively used for dye degradation (Mardikar *et al*, 2021). IONPs have lately been utilized in the elimination of color contamination, thanks to the expanding popularity of nanotechnologies. Diagnostic imaging, magnetic fluids, biological separation, pharmaceutical administration, magnetic storage media, solar energy transformation, the electronics industry, and catalysts are just a few of the applications for IONPs, if amorphous or crystalline. There were various researches on the synthesis of crystalline IONPs utilizing physical and chemical approaches, yet, because of the high cooling rate needed, there were some researches on preparing amorphous IONPs. Because it has a cooling rate of over 10 million degrees per second, the sonochemical technique is the most frequent utilized approach for generating amorphous IONPs (Nath and Banerjee, 2013).

FeCl₃, Fe(CO)₅, Fe(OAc)₂, Fe(NO₃)₃, and Fe(OEt)₃ are used as precursors in sonochemical processes for iron oxides (Phu *et al*, 2011). Amorphous IONPs have also been created using other methods like microwave heating and electrochemical synthesis. Because microwave heating does not necessitate complex systems, it has piqued the interest of scientists, Microwaves operate as high-frequency electric fields in microwave heating, heating any substance having movable electric charges, such as polar molecules in a fluid or conducting ions in a solid, Polar solvents heat up because their constituent molecules are forced to spin with field and lose energy in collisions, Microwave radiation is effectively transferred to heat, allowing for superheating at ambient pressure and amorphous material nucleation in a short time.

Nanoparticles from natural or biological systems are highly important in nature and industrial applications. In contrast to chemical synthesis, the nanoparticles obtained from biological systems such as fungi, bacteria and plants are economic and eco-friendly. The nano-particles possessing high surface area, good catalytic biocompatibility, and a high fraction of surface atoms are expected to be potential with distinctive capacity (Bhattacharya and Gupta, 2005).

Actinobacteria are ecologically and biotechnologically important group of microorganisms due to their high capacity to synthesize a wide range of enzymes and bioactive metabolites (Lee *et al*, 2020). In addition, actinobacteria isolated from different ecosystems have been recognized as the potential synthesizers of metal nanoparticles (Manivasagan *et al*, 2016). Nanomaterials with unique sizes and

structures are expected to find various novel applications and their discovery by using biological sources such as actinobacteria may pave the way to novel materials, processes, and phenomena at the nanoscale, as well as the development of new experimental and theoretical techniques for research.

A highly prospective and well developed environmental applications of the nanotechnology is the treatment and remediation of the water, where the nano-materials purify the water with use of various mechanisms, which include the adsorption of the heavy toxic metals, harmful compounds and other pollutants, removing and inactivation the pathogens, and transformation of toxic materials to compounds of lower toxicity (Ghasemzadeh *et al*, 2014). One of the most widely utilized adsorbents for environmental remediation is nano-iron (Fe NPs) by virtue of its abundance of reactive surface sites and high reactivity. Iron nanoparticles (Fe-NPs) are widely experimented for a wide range the biological applications as a result of its high values of magnetization and uniform physicochemical properties (Frey *et al*, 2009). In this study, iron nanoparticles will be synthesized using soil actinobacteria and their potential to remove heavy metals from water will be investigated.

2. NANOTECHNOLOGY

Nanotechnology and nanoscience are the application and study of very small objects, and those might be applied in biology, chemistry, materials science, engineering and physics, among other subjects. The concepts and ideas behind nanotechnology and nanoscience has begun with physicist R. Feynman's talk "There's Plenty of Room at the Bottom" at an American Physical Society meeting at the California Institute of Technology (CalTech) on Dec. 29th, 1959, long before the term "nanotechnology" has been coined, Feynman had proposed an approach by which the scientists could alter and control individual atoms and molecules in his talk. Professor N. Taniguchi had presented the term nanotechnology over a 10 years later while researching ultra-precision machining. The modern nanotechnology had only begun in 1981, with the development of the scanning tunneling microscope, which could "see" individual atoms. "Nanotechnology" is derived from the Greek word "dwarf." The prefix "nano" stands for 1 billionth of a prefix. One billionth of a meter, or 100,000th of the width of a human hair, is a nanometer. Until IBM in Switzerland developed a new generation of microscopes in the 1980s, the world of molecules and atoms cannot be manipulated or observed. Individual atoms react comparably to structures less than a nanometer in size, however materials hundreds of nanometers in size or more exhibit continuous features. Nanoscale behaviors and characteristics may be exceedingly different due to varying chemical and physical interactions. Interfaces and surfaces, along with the physical confinement of energy and matter, have the ability to influence virtually all material properties (chemical, physical, optical, etc.), leading to amazing new behaviors. The creation of light from dark materials, along with the enhancement of catalyst efficiency, are two examples.

2.1. Applications and Benefits of Nanotechnology

NP applications are delivering on nanotechnology's promises to enhance society in both unexpected and expected ways after more than two decades of main nanoscience research and over five decades of focused R&D under the national nanotechnology initiative Homeland security, information technology, transportation, medical, consumer protection, energy, and environmental research are just a few of the industrial and technical areas that take advantage from nanotechnology (Figure 2.1). Various nanotechnology's advantages depend on the ability to control material formations at very small scales to obtain desired qualities, thus expanding the materials

science toolkit. Materials may be made lighter, stronger, more durable, sieve-like reactive, and better electrical insulators with the use of nanotechnology, among other things. Different everyday commercial items that depend on materials and nanotechnologies are available (Castro *et al*, 2014).

Nano-sized fabric additives or surface treatments in personal body armor can provide lightweight ballistic energy deflection along with resistance to staining, wrinkling, and bacterial growth. In addition, clear nanoscale films can be used to make eyeglasses, camera and computer displays, windows, and other surfaces water and residue repellent, self-cleaning, antireflective, UV or infrared light resistant, antimicrobial, anti-fog, electrically conductive, or scratch-resistant (Karkare, 2010).

Nanoscale materials enable reusable, long-lasting "smart textiles" with flexible nanoscale sensors and electronics for the monitoring systems, renewable energy harvesting, and energy harvesting through movement (Yan *et al*, 2020).

Less-weighted trucks, cars, boats, planes, and spacecraft could save a lot of fuel. Nanoscale additions in polymer composite materials have been utilized in the tennis rackets, baseball bats, motorcycle helmets, bicycles, luggage, automotive components, and power tool housings for making them rigid, lightweight, resilient, and robust. Carbon nanotube CNT sheets are already being produced in preparation for future air vehicles. Because of their light weight and high conductivity, they're optimal for applications like the electro-magnetic shielding and thermal management (Loos, 2014).

Enzyme nano-bioengineering has been aimed to facilitate conversion of the cellulose from wood chips, maize stalks, unfertilized perennial grasses, and other sources into ethanol for energy. Electronics, construction, health care, packaging, food, energy, automotive, and military are just a few of the industries where cellulosic nanomaterials have shown potential. Cellulosic nanoparticles are expected to be less costly than many other nanomaterials, and they have a remarkable strength-to-weight ratio, among other things. High-power rechargeable battery systems, thermo-electric materials for temperature control, inexpensive/high-efficiency electronics and sensors, tires with lower rolling resistance, thin-film smart solar panels, and fuel additives for the cleaner exhaust and extended range are all examples of nano-engineered materials in automotive products (Saravanavel, 2018).

Nanostructured ceramic coatings for machine parts are far more durable compared to the conventional wear-resistant coating. Nanotechnology-enabled lubricants and motor oils decrease the wear and tear as well, allowing moving parts in everything from the power tools to the industrial gear to last longer (Saravanel, 2018).

Catalysis with NPs is becoming more popular as a way to speed up chemical reactions, which lowers the number of catalytic materials that are required to achieve the required outcomes, lowering pollution and saving money, Petroleum refinery and automotive catalytic converters are two major applications (Lanzafame *et al*, 2017).

Stain removers and degreasers, air purifiers, environmental sensors, and filters, antibacterial cleansers, and specialty paints and sealing solutions, like self-cleaning home paints which resist dirt and stains, are all made with nano-engineered materials (Jagessar, 2021).

Nanoscale materials are also being used for improving the performance regarding various personal care items. For years, nanoscale zinc oxide and titanium dioxide were employed in sunscreen to give sun protection, whereas remaining virtually invisible on the skin (Pathak *et al*, 2018).

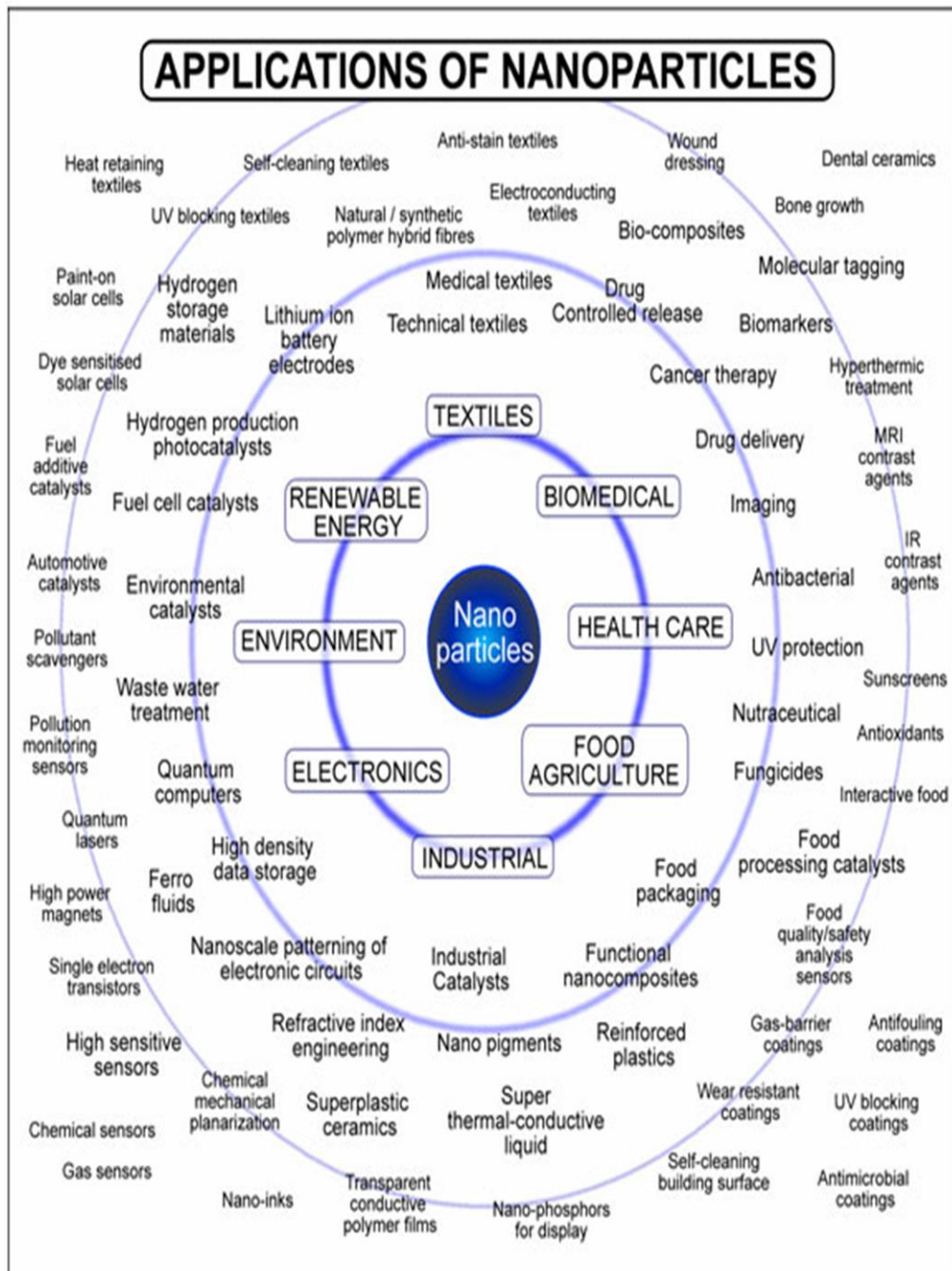


Figure 2.1. Application fields of nanotechnology

2.2. Environmental Nanotechnology

Environmental nanotechnology is widely regarded as having a significant impact on present environmental engineering and science. Also, the nanoscale has aided creating and implementing an inexpensive and new approaches for pollution remediation, monitoring, detection, and remediation. Biosensors made of nanostructured materials are utilized for monitoring and detecting various compounds. Due to the substantially higher surface area of NPs on a mass basis, using NP might offer an advantage over traditional methods. A few NPs are adsorbent of pollutants due to their distinctive electronic and structure characteristics (Zhang *et al*, 2019). Various nanomaterials have adsorption characteristics that vary in size. Chemically-modified nanomaterials, particularly nano-porous materials, have gotten a lot of attention as a result of their large surface area. Yet, the particle size related to these materials is typically 10-100 μm , not nano-range. Another possibility is to chemically alter the NP. The capacity of TiO_2 functionalized with ethylenediamine for removing anionic metals from contaminated groundwater was investigated (Kyzas *et al*, 2013).

Carbon adsorption, air stripping, oxidation by chlorination or ozonation, ultrafiltration, incineration, and sedimentation are some of the most prevalent environmental remediation processes utilized for treating significant volumes of water meant for municipal water systems. Those methods are commonly employed to remove pollutants on a wide scale. On a lesser scale, activated carbon adsorbents are being used for removing organic contaminants at the point of application. Technical and scientific approaches for reducing pollution depend on a variety of methodologies, which differ in the cases of soil, water, and air purification. The method of remediation is determined by the complexity and character of the contaminated media, as well as the treatment's economic costs, The decision to use a specific technology is heavily influenced by environmental remediation (Ilyas *et al*, 2019).

2.2.1. Application in Environment

Nanotechnologies are already interacting with the environment. Scientists and engineers are manipulating matter at the nanoscale, and these nanoscale processes and products are being used by industry in commercially available products. These products are either applied directly to the environment or end up in the environment through indirect pathways.

Engineered NPs are increasingly being employed in home and industrial applications, leading to their release into the environment. Knowing the reactivity, mobility, persistence, and ecotoxicity of such NPs in the environment is critical for determining their environmental risk. The usage of engineering materials has a potential to reduce the NP concentrations in the soil and the groundwater, which makes it one of the most relevant exposure channels for analyzing environmental problems. As a result of their high surface to mass ratio, the natural NPs are critical in solid/water partitioning. In addition, pollutants might be absorbed onto the surface of the nanoparticles, which have been co-precipitated throughout natural NP formation, or restricted via NP aggregation with pollutants adsorbed on their surface. Pollutant interactions with NPs are influenced by their composition, size, porosity, shape, aggregation/disaggregation, and aggregate structure (Levard *et al*, 2012).

Due to their negative impacts on human health and environment, heavy metals like lead, mercury, cadmium, thallium, and arsenic were removed from the natural water. For this hazardous soft material, superparamagnetic iron oxide NPs represent a sufficient sorbent material, Because of the lack of the analytical technologies that are able to quantify the trace concentrations of the NPs, no measurements of the designed NPs in environment have been provided (Mueller and Nowack, 2008). Photodegradation via NPs is a widespread procedure as well, and a variety of nanomaterials are used for this. For photodegradation, Rogozea *et al.* (2016) employed NiO/ZnO NPs modified silica in a tandem method. The effective photodegradation reaction was aided by the high surface area regarding NPs because of their small size (less than 10 nm). Furthermore, the same group has indicated the synthesis of a wide range of NPs as well as their fluorescence, optical, and degradation applications (Mourdikoudis *et al*, 2018).

2.3. Approaches of Synthesis of the Nano-Materials

Nanostructure materials had gained much attention since their chemical, physical, magnetic, and electronic characteristics considerably differ from their higher-dimensional counterparts and are affected by their size and form. Various strategies for the synthesis and fabrication of the nanostructure materials with controlled size, shape, structure, and dimensionality were established (Sajanlal *et al*, 2011).

As indicated in (Figure 2.2) there are two general ways to nanomaterial synthesis:

- a) Top- down approach
- b) Bottom–up approach.

(a) Top-down strategy: this approach involves decreasing bulk materials to nanoscale particles or structures. Methods for creating top-down synthesis are an extension of the ones that are utilized to make micron-sized particles. Also, top-down approaches are fundamentally simpler, relying on bulk material removal or division, or bulk manufacturing process downsizing, to build the needed structure with acceptable characteristics. The most considerable issues that is related to this strategy is the inaccuracy of the surface structure. Nanowires created through lithography, for instance, are not always smooth and can have many structural flaws and impurities on their surface. High-energy wet ball milling, atomic force manipulation, electron beam lithography, aerosol spray, gas-phase condensation, and other processes are examples (Usman *et al*, 2020).

(b) Bottom-up strategy: This strategy is a substitute that has a potential for producing less waste and therefore have higher cost-effectiveness.

The molecule-by-molecule, atom-by-atom, or cluster-by-cluster constructions of the material are known as the bottom-up approach.

Several of such methods are still under development or are only now being utilized for the commercial nano-powder manufacture.

A few of common bottom–up approaches that have been indicated for the manufacture of luminescent NPs include oraganometallic chemical route, sol–gel synthesis, revere-micelle route, colloidal precipitation, hydrothermal synthesis, electrodeposition, template assisted sol–gel, etc (Usman *et al*, 2020).

Bottom-up, or self-assembly, techniques to nanofabrication combine simple units into bigger structures using physical or chemical forces operating at the nanoscale. Bottom-up approaches are becoming an increasingly significant complement to top-down approaches in nanofabrication as component sizes decreases. Biological systems, in which nature has harnessed chemical forces to generate practically all of the structures required for life, provide inspiration for bottom-up

approaches. Nature's capability to form small clusters of certain atoms, which might subsequently self-assemble into more complex structures, is hoped to be replicated by researchers (Biswas *et al*, 2012).

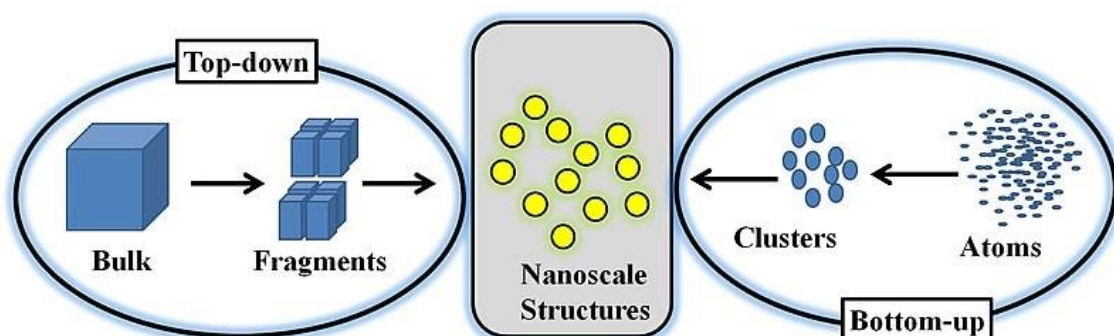


Figure 2.2. Two approaches for nanoparticles synthesis

2.4. Green Nanotechnology

Green nanotechnology can be defined as a one of the green technology types incorporating green engineering and green chemistry. It saves gasoline and energy by using fewer renewable inputs and materials whenever possible. Nanotechnology processes, products, and applications are also expected to play significant role in the climate and environmental protection through the conservation of the energy, water and raw materials, along with the reduction of hazardous waste and green-house gas emissions (Maksimović and Omanović-Miklićanin, 2017). Green nano-technology has several significant benefits, including an increase in energy consumption, a decrease in pollution and greenhouse gas emissions, and decreased usage of non-renewable raw materials. Green nanotechnology offers a tremendous opportunity to prevent harmful consequences from occurring in the first place. Green nanotechnology is specified as one of the technology types for enhancing the environmental sustainability of operations which cause negative externalities, like the production of green nano-goods. Green nanotechnology is defined as the development of clean approaches that employ green nanotechnology to reduce potential human health and environmental risks (Maksimović and Omanović-Miklićanin, 2017).

2.5. Characterization of NPs

There are considerable obstacles in analyzing nanomaterials due to the multidisciplinary nature of the field, the issues related to sample preparation for analysis, the non-existence of reliable reference materials for the calibration of

analytical equipment, along with the interpretation of findings (Mourdikoudis *et al*, 2018). The characterization of NPs faces considerable challenges, like determining their concentration on-line and in situ, especially in scaled-up manufacturing, and studying them in complex matrices. Large-scale manufacturing waste and wastewater must be monitored as well. With the scaling up of NP manufacturing, more precise measurement methods will be required. Therefore, it is crucial to explain nanomaterials produced in various ways as thoroughly as possible. We're interested in not just the physical properties regarding the NP core, yet also the surface ligands influencing them.

For the examination of different physicochemical characteristics of NPs, numerous characterization methods have been used. X-ray photoelectron spectroscopy, X-ray diffraction analysis, transmission electron microscopy, scanning electron microscope, BET, and particle size analysis are examples of such approaches.

One of the most commonly utilized approaches for characterizing NPs is XRD. Generally, XRD yields information on crystalline structure, lattice parameters, phase nature, and crystalline grain size. The Scherrer equation is used to calculate the latter parameter that has been based upon broadening regarding the most intense XRD measurement peak for a certain sample. XRD approaches, which are often utilized in the powdered form after drying their respective colloidal solutions, have an advantage of the production of the statistically representative, volume-average values. Through the comparison of the intensity and positions of the peaks with the reference patterns provided from International Centre for Diffraction Data, the composition of the particles may be established (Londoño-Restrepo *et al*, 2019).

DLS is a prominent approach for assessing the size of NPs in colloidal fluids at the nano- and sub-micron scales, The NPs distributed in a colloidal solution preserve Brownian motion. DLS identifies light scattering as a function of time, which is after that utilized to compute the NP hydrodynamic diameter in liquid using the Stokes–Einstein hypothesis, To avoid multiple scattering in DLS, a low NP concentration is needed (Caputo *et al*, 2021).

SEM/EDS is an abbreviation for Scanning Electron Microscopy with Energy Dispersive Spectroscopy. With the use of the SEM/EDS Microscope System, we may examine nano- and micro-scale characteristics with magnifications up to 300,000x and

determine chemical elemental composition on or in surface of testing sample. This technological investment expands our current capabilities to provide you with a comprehensive testing package that includes cross-sectional imaging, surface analysis, fatigue and corrosion testing, and SEM. SEM advancements now allow for high-resolution imaging of single nanoparticles (NPs) with diameters considerably below 10 nm (Hodoroaba *et al*, 2016).

Characterization of nanoscale materials is also done using the Brunauer–Emmett–Teller (BET) approach. It was named after the initials of the developers' surnames, Emmett, Brunauer, and Teller, and depend on the principle of physical adsorption of a gas on the solid surface.

It is extensively used to determine the surface area of nanostructures since it is a generally quick, accurate, and simple approach (Wang, 2008).

There are many other tests such as photoluminescence (PL) spectroscopy, nanoparticle tracking analysis (NTA), mass spectrometry (MS) (Mourdikoudis *et al*, 2018).

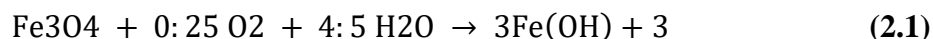
2.6. Iron nanoparticles

The usage of nano-based adsorbents is considered as one of the more convenient ways for extracting heavy metals from wastewater systems. Iron oxide-based nanomaterials are more desirable for removing heavy metal pollution from water due to their major properties like huge surface area, small size, and magnetic property. IONPs' magnetic properties enable for easy removal of adsorbents from the system, which might after that be reused. The cost burden is reduced by the reusability regarding iron oxide-based nanomaterials (Marooufpour *et al*, 2019).

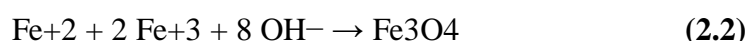
The synthesis of IONPs is being worked on intensely, not only for their major science curiosity, but also for their potential applications in a variety of disciplines. Due to their large surface area, tiny size, and magnetic capability, the use of iron oxide-based nanomaterials with unique properties and functionalities has recently received a lot of attention. The synthesis of iron oxide nanoparticles has received substantial attention. As shown in (Figure 2.3), iron oxide nanoparticles are generated using three different methods: physical, chemical, and biological. Chemical techniques are well-known and well recognized ways for producing iron oxide nanoparticles in large quantities. As shown in (Figure 2.3) various chemical processes were recorded in the

literature, including thermal decomposition, chemical co-precipitation, sol-gel, and electrochemical (Bhattacharya, 2016).

The chemical coprecipitation technique is a commonly used approach for the production of IONPs. A stoichiometric mix of ferrous and ferric salts in the ratio (2:1) ($\text{Fe}^{3+}/\text{Fe}^{2+}$) is produced in an aqueous medium with the existence of base and lack of oxygen using the chemical coprecipitation process displays the whole process of Fe_3O_4 production at pH levels in range of (8-14), Fe_3O_4 might also oxidase as :



With the existence of acid and oxygen, magnetite NPs are converted to hematite NPs. The main benefit of this approach is the fact that it produces a large material volume, whereas allowing for fine control of particle size (2 nm–20 nm) and form via ionic strength, pH, and solution concentration. The thermal decomposition technique can be used to make iron oleate with organic solvents and surfactants, from the high-temperature breakdown of iron precursors, like $\text{Fe}(\text{CO})_5$, $\text{Fe}(\text{Cup})_3$, and $\text{Fe}(\text{acac})_3$. The thermal breakdown method has the advantage of allowing more control over the shape and size of IONPs. The shape and size of IONPs are influenced by the temperature and precursor. Hydrothermal employs iron precursors through using high pressure and heat to water. Reactions are performed in autoclaves or reactors. In hydrothermal circumstances, mixed metal hydroxides were hydrolyzed and oxidized, then neutralized, resulting in the production of NPs. A hydrothermal technique has been used to make ferromagnetic Fe_3O_4 NPs with a diameter of 27 nm with the existence of a surfactant sodium bis(2-ethylhexyl) sulfosuccinate. The hydrothermal approach was used to make aqueous ferrofluid IONPs utilizing citric acid as a reducing agent. The particles are around 8 nm in size. The hydrothermal approach was also used for preparing surface modification of IONPs with polyethyleneimine.



To comprehend the behavior that is related to colloidal ferrofluid particles and enhance their applicability, comprehensive research into their fluid stability is required. In the aqueous and biological systems, iron oxide nanoparticles easily aggregate. Because of the presence of hydroxyl groups, IONPs have a hydrophilic surface. Other techniques for preparing IONPs are indicated in (Figure 2.3).

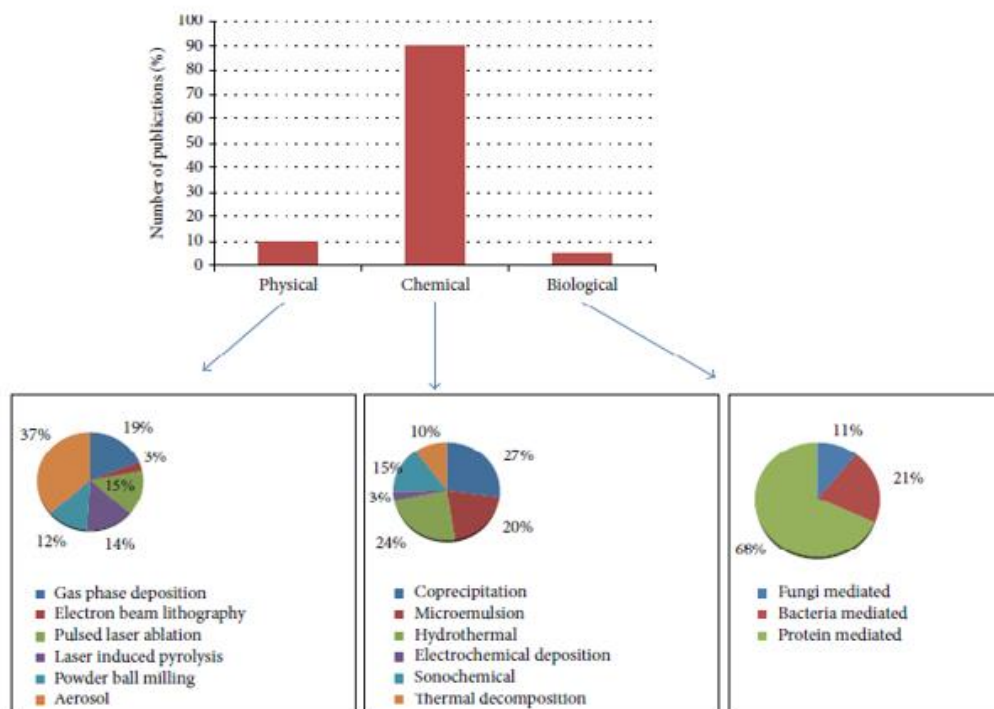


Figure 2.3. Various methods of preparation of nanoparticles

There is hydrophilic contact between the particles, and such particles agglomerate to form huge clusters. There must be a balance of attracting and repulsive forces acting between nanoparticles for stability. To address this issue, IONPs must have both electrical and steric stability. The existence of hydroxyl groups on IONPs surface makes it one of the useful synthetic tools for attaching various functions. Surface modification techniques for IONPs increased material stability and provided unique properties. The stability of iron oxide particles is critical for the production of magnetic colloidal "ferro fluids". Those ferrofluids are stable against the aqueous, biological media and magnetic field (Moerz *et al*, 2015).

MRI, drug administration, cellular labeling, hyperthermia, environmental cleanup, and protein separation, are just a few of the biological applications for modified magnetic NPs. Figure 5 displays the many ways to INOP manufacturing that were documented. Attaching alkoxy silane to the IONP surface with different silane coupling agents has been considered as the most common method for the surface modification. Organosilane can be defined as one of the appealing reagents for surface modification of NPs due to its low commercial availability, simple synthetic technique for immobilizing on the NP's surface, and wide variety of activity. The surface hydroxyl group of the IONPs reacts with the Si-OR group of silane. It is a condensation

and hydrolysis process (Figure 2.4). Also, the trialkoxy silane functional group aids in the introduction of various functionalities like azide, amine, thio, aldehyde, hydroxyl, halide, and acid on IONP surface. Silane coupling agents are also useful for attaching small organic compounds, polymers, and biomolecules to surfaces. PEG is used to modify the surface of INOPs via 3-aminopropyl triethoxysilane PEG NPs with a molecular weight greater than 1000gm/mL created stable NPs. Silane-PEG is used to encapsulate magnetic NPs. For MRI of murine tumors, oleic acid on the surface related to IONPs was substituted through a bio-compatible silane PEG polymer (Misk and Franco, 2011).

The surface modification regarding magnetic NPs through coating with silica was indicated via Ahangaran et al. NPs simply agglomerate due to their hydrophilic nature. Vinyltriethoxysilane works as a coupling agent, making the surface more hydrophobic and reducing agglomeration. On the surface of Fe₃O₄, cyanoethyl triethoxysilane is immobilized. The cyano group on the surface of the magnetite NPs stabilizes them and promotes cell targeting and cellular labeling. IONP modification can also be accomplished by click chemistry (Figure 2.4). The surface of magnetic NPs is modified by click reactions like thio-ene, azide-alkyne, diels-alder, and thio-yne. SPINOs have oligonucleotides immobilized on their surfaces. The click reaction between oligonucleotides bearing alkyne and alkyne-containing oligonucleotides is mediated by azide-alkyne copper (Dave and Chopda, 2014).

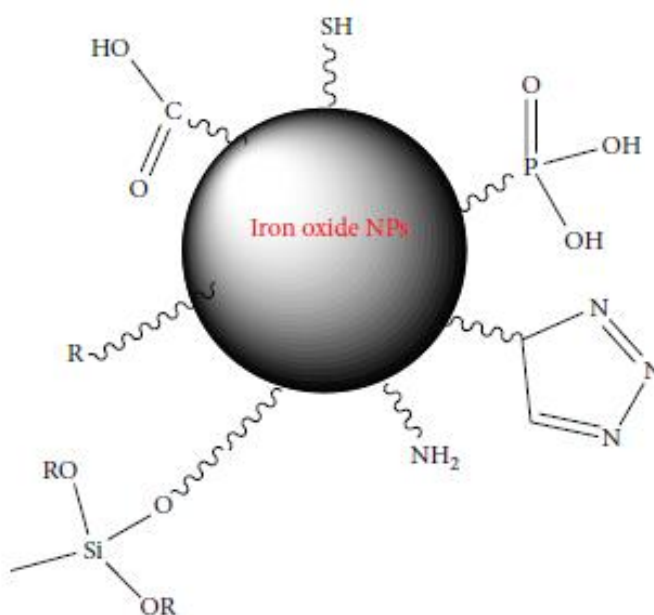


Figure 2.4. Iron oxide nanoparticles

2.7. Biogenic Synthesis

Microorganisms have the ability to create a broad variety of the nanostructure types. This had triggered the scientists' curiosity in the use of such microbes for synthesizing nano-structures for various applications. Fungi and bacteria might produce inorganic molecules through the biologically induced and mediated synthesis. Nano-structures with desired composition and geometrics might produced through directing biological synthesis. Biological NP synthesis is still constrained with regard to particle geometric controllability and process scalability, notwithstanding the accuracy of NP physicochemical synthesis. Biologically-induced synthesis, on the other hand, has allowed scientists to make inorganic NPs from common metal precursors with various compositions. Microorganisms including fungi, bacteria, and algae are more and more employed to make nanosize particles. There are many distinct microbes which create the NPs by differently reacting with metal precursors. Fungi and bacteria, for instance, can produce intracellularly and extracellularly, and both activities follow various paths in various microbes. Intra-cellular synthesis uses metal ions through the cell wall, with positive-charge ions interacting with negative-charge wall. Metal NPs are formed when such ions are reduced by enzymes in the cells (Zikalala *et al*, 2018).

Metal NP production through microorganisms is an environmentally friendly and green technology. Gold, silver, zirconium, platinum, iron, palladium, metal oxides, and cadmium like zinc oxide and titanium oxide are all made by microorganisms, such as actinobacteria.

2.8. Actinobacteria

Actinobacteria are found in both marine and land environments, majorly in soil, in which they play a significant part in the recycling regarding refractory biomaterials through digesting complex polymer combinations in dead animals and plants, along with fungal components. Significant microorganisms which are employed to make secondary metabolites are considered biotechnological processes. Over 10000 bio-active metabolites are created by the actinobacteria, responsible for 45% of all the bio-active microbial metabolites that have been discovered. In particularly, *Streptomyces* species, produce industrially significant micro-organisms due to their abundance of

helpful bioactive natural compounds with potential applications (Dhanasekaran and Jiang, 2016).

Actinobacteria are Gram-positive bacteria having a high GC DNA concentration. Also, they are one of the major bacterial phyla, and they might be identified in the terrestrial as well as the aquatic environments. Various actinobacteria reside in mycelial communities and have a wide range of morphologies. Also, they have a complicated secondary metabolism, producing over 2/3 of all of the naturally-derived antibiotics currently in clinical use, along with a variety of anthelmintic, anticancer, and antifungal chemicals. Therefore, medicine, biotechnology, and agriculture all rely on such bacteria. Pathogens (notably, *Mycobacterium*, *Corynebacterium*, *Propionibacterium*, *Nocardia*, and *Tropheryma* species), soil inhabitants (*Streptomyces* species and *Micromonospora*), plant commensals (such as *Frankia* spp.), and gastrointestinal commensals (*Bifidobacterium* spp.) are all members of the *Actinobacteria* phylum (Ventura *et al*, 2007).

Actinobacteria sporulate through segmentation and fragmentation or conidia generation, whereas they reproduce via binary fission or through generating conidia or spores. Actinobacteria have a compact, leathery morphology, a conical appearance on culture media with dry surface, and are usually covered by the aerial mycelium (Dhanasekaran and Jiang, 2016), (Figure 2.5).

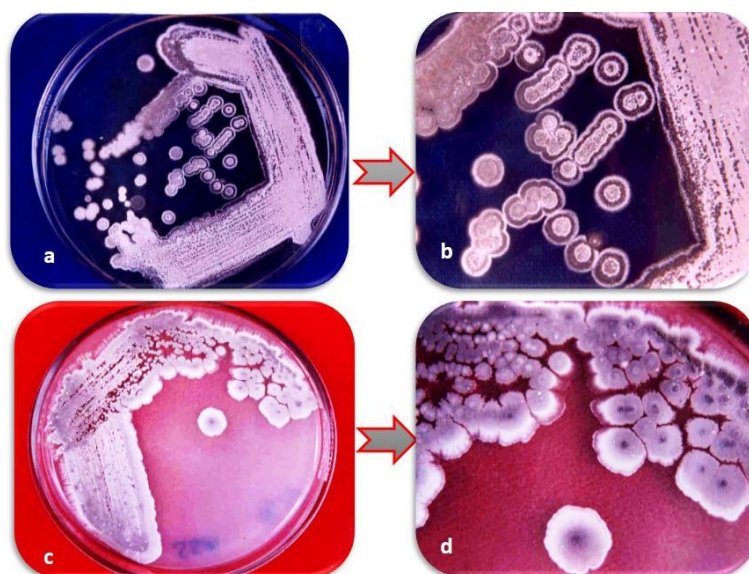


Figure 2.5. Actinobacteria isolate appearance on the Starch casein agar plate. a, c Plate view of the isolates of the Actinobacterial. b, d Morphology of the individual colonies (Anandan *et al*, 2016).

Actinobacteria are well-known for creating secondary and primary metabolites having important applications in a variety of the areas. They are also a potential source of a variety of the essential mass-produced enzyme types, Antibiotics derived from Actinobacteria account for a significant share of the market. They develop cancer-fighting enzyme inhibitors and immunomodulators which increase immune response. A wide range of insecticides, hydro-carbons, aromatic and aliphatic chemicals might be decomposed by them. They work in the field of microbial transformations of organic molecules, which is a lucrative industry. Various Actinobacteria genera have the ability to convert underutilized urban and agricultural wastes into high-value chemical compounds through bioconversion. Plant biotechnology benefits from actinobacteria due to the fact that the strains with antagonistic activities against the plant diseases might be employed for bio-control. Their metabolic potential opens up a lot of possibilities for research (Dhanasekaran and Jiang, 2016).

2.9. Biological NP Synthesis by Actinobacteria

Inorganic compounds are produced by actinobacteria either extracellularly or intracellularly, and are often nanoscale in shape and dimension. Chemical detoxification and energy-dependent ion efflux from the cell via membrane proteins such as chemiosmotic cation, ATPase, or proton anti-transporters are the most dangerous forms of heavy metal resistance in actinobacteria. Changes in solubility have an impact on microbial resistance. This is why the microbial systems might detoxify the metal ions through converting soluble harmful inorganic ions into non-toxic metal nano-clusters. Actinobacterial detoxification can take the form of extra-cellular bio-mineralization, complexation, bio-sorption, or precipitation, along with intra-cellular bio-accumulation. Metal NPs made produced extracellularly have additional commercial applications. Since polydispersity is the main problem, it's crucial for the optimization of conditions for the mono-dispersity in a biological procedure. The accumulating particles in the case of intracellular production have a specified diameter and a smaller polydispersity (Manivasagan *et al*, 2016).

2.10. Heavy Metals

Heavy metals are well-known environmental pollutants because of their toxicity, persistence in the environment, and bioaccumulative nature. Their natural sources include weathering of metal-bearing rocks and volcanic eruptions, while

anthropogenic sources include mining and various industrial and agricultural activities. Mining and industrial processing for extraction of mineral resources and their subsequent applications for industrial, agricultural, and economic development has led to an increase in the mobilization of these elements in the environment and disturbance of their biogeochemical cycles. Contamination of aquatic and terrestrial ecosystems with toxic heavy metals is an environmental problem of public health concern. Being persistent pollutants, heavy metals accumulate in the environment and consequently contaminate the food chains. Accumulation of potentially toxic heavy metals in biota causes a potential health threat to their consumers including humans (Smith *et al*, 2013). Cadmium compounds are currently mainly used in re-chargeable nickel–cadmium batteries. Cadmium emissions have increased dramatically during the 20th century, one reason being that cadmium-containing products are rarely recycled, but often dumped together with household waste. Cigarette smoking is a major source of cadmium exposure. In non-smokers, food is the most important source of cadmium exposure. Recent data indicate that adverse health effects of cadmium exposure may occur at lower exposure levels than previously anticipated, primarily in the form of kidney damage but possibly also bone effects and fractures. Many individuals in Europe already exceed these exposure levels and the margin is very narrow for large groups. Therefore, measures should be taken to reduce cadmium exposure in the general population in order to minimize the risk of adverse health effects (Järup, 2003).

The general population is exposed to lead from air and food in roughly equal proportions. During the last century, lead emissions to ambient air have caused considerable pollution, mainly due to lead emissions from petrol. Children are particularly susceptible to lead exposure due to high gastrointestinal uptake and the permeable blood–brain barrier. Blood levels in children should be reduced below the levels so far considered acceptable, recent data indicating that there may be neurotoxic effects of lead at lower levels of exposure than previously anticipated. Although lead in petrol has dramatically decreased over the last decades, thereby reducing environmental exposure, phasing out any remaining uses of lead additives in motor fuels should be encouraged. The use of lead-based paints should be abandoned, and lead should not be used in food containers. In particular, the public should be aware of glazed food containers, which may leach lead into food. For the reasons mentioned earlier, in this study, lead and cadmium metals were selected and tested for their

removal by a nanobiological method using iron nanoparticles synthesized by actinobacteria and acting by adsorption, sorption and other mechanisms.

3. MATERIALS AND METHOD

3.1. Selective Isolation of Actinobacteria

Five soil samples were collected from Turkey and Iraq (figure 3.1). The samples were taken at 10 cm depth from the ground surface using sterile polypropylene tubes and transferred to the laboratory. The soil samples were stored at ambient temperature for 3 days. One gram from each soil sample was suspended in 9 ml of ¼ strength Ringer's solution and mixed (with glass ball) until the mixture becomes homogeneous. The soil suspensions were pre-treated by heating at 60°C for 20 min in a water bath, and then, the suspensions were further diluted to prepare 10⁻² and 10⁻³ suspensions. Then, 0.1 ml from each suspension was spread over actinomycete isolation agar, Czapek-Dox agar and starch-casein agar media supplemented with nalidixic acid (10 µg/ml) and cycloheximide (50 µg/ml) to prevent fast-growing bacteria and fungi, respectively (Amkraz *et al*, 2010) . The inoculated agar plates were incubated at 28 °C for three weeks. Actinobacteria-like colonies were selected and purified on glucose-yeast extract-malt extract agar and tryptone-yeast extract-glucose agar media. The purified isolates were maintained in glycerol stock solutions (25%, v:v) at -20°C.

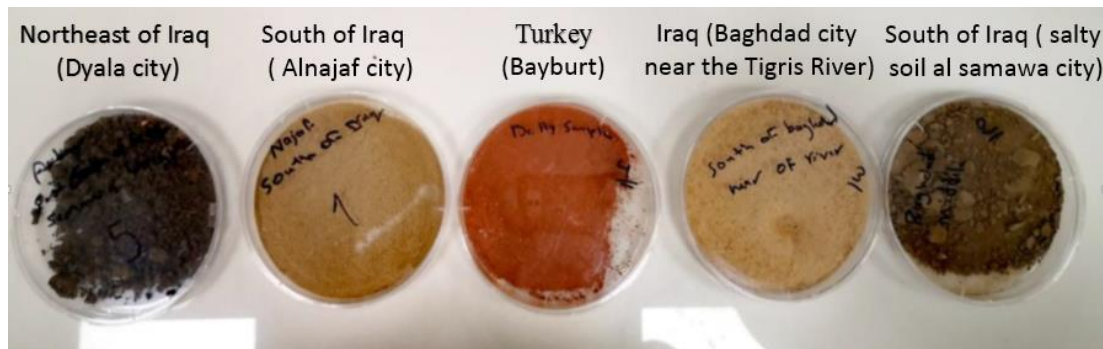


Figure 3.1. Soil samples

A set of culture media was used for the previous steps, namely:

- Yeast extract agar (Mohamed *et al*, 2017)
- CZAPEK peptone agar (Lapage *et al*, 1970)
- GYM Streptomyces medium (Ay, 2021)
- Tryptone yeast extract agar (Sheikh *et al*, 2019)
- ISP medium 2 with NaCl 5% (Vijayakumar *et al*, 2010)

For subculturing and checked the purity of the each isolate, all of those medium pH adjusted on 7.2

3.2. Identification of Bacterial Isolates

A total of six isolates producing iron oxide nanoparticles were selected based on their morphological characteristics such as colour of substrate and aerial mycelia. The isolates were identified based on pairwise comparison of the 16S rRNA gene sequences. Firstly, the genomic DNA of each isolate was extracted using Purelink Genomic Isolation Kit (Invitrogen) using the manufacturer's instructions:

1. At 37°C and 55°C, two heat blocks were prepared.
2. Lysozyme Digestion Buffer (EDTA, Tris, hydrochloride,X) was prepared (to approximately 200µL Lysozyme Digestion Buffer/sample, fresh Lysozyme is added for obtaining a final concentration of the Lysozyme of 20mg/mL).
3. With the use of a wood stick, the bacteria colonies from the petri dish were transferred into the Eppendorf tubes.
4. 180µL of the Lysozyme Digestion Buffer that contains the Lysozyme was added and mixed well through brief vortexing.
5. Incubated for 30 min in a dry bath at 37°C.
6. Triton X-100 was added to the cell lysates, mixed, and incubated for 30 min at 37°C.
7. 20 µL Proteinase K was added and mixed well with brief vortexing.
8. 200 µL of the PureLink® Genomic Lysis/Binding Buffer was added and mixed well with brief vortexing.
9. Incubation at 55°C for 30 min.
10. 200 µL 96–100% ethanol was added to lysate. Mixed thoroughly through vortexing for 5 sec in order to yield homogenous solution, after that, centrifuged 10,000xg for 1 min.
11. PureLink® Spin Column was removed in a Collection Tube from a package.
12. Lysate (about 640µL) that has been prepared with the PureLink® Genomic Lysis/Binding Buffer and ethanol was added to PureLink® Spin Column.

13. The column was centrifuged at $10000 \times g$ for 1 min at the temperature of the room.
14. The collection tube was discarded and spin column was placed into clean PureLink® Collecting Tube provided in the kit.
15. 500 μ L of the washing Buffer 1 was added into the column.
16. The column was centrifuged at room temperature at $10000 \times g$ for 1 min.
17. The collection tube was discarded and the spin column was placed in a clean PureLink® tube of collection.
18. 500 μ L of the Washing Buffer 2 was added into the column.
19. The column was centrifuged at maximal speed (15000 rpm) for 3 min at the room temperature. The collection tube was discarded.
20. The spin column was placed in sterile 1.5mL micro-centrifuge tube.
21. 50 μ L of the PureLink® Genomic Elution Buffer was added into the column.
22. Incubation at the room temperature for 1 min. Centrifuge column at the maximal speed (15000 rpm) for 1 min at the room temperature. The tube includes the purified genomic DNA.

The 16S rRNA genes from pure cultures were amplified using the universal primers 27F (5'-AGAGTTTGATC(AC)TGGCTCAG-3') and 1525R (5'-AAGGAGGTGWTCCARCC-3') under following PCR conditions: pre-denaturation at 94°C (2 min), 35 cycles for denaturation at 94°C (1 min), annealing at 55°C (2 min) and extension at 72°C (3 min). The PCR products were purified and sequenced by Macrogen Inc. (The Netherlands) using the primers 518F (5'-CCAGCAGCCGCGGTAATACG-3'), 800R (5'-TACCAGGGTATCTAATCC-3') and MG5F (5'-AAACTCAAAGGAATTGACGG-3') on an ABI PRISM 3730 XL automatic sequencer. The 16S rRNA gene sequence data for each isolate was deposited in GenBank (<https://www.ncbi.nlm.nih.gov/genbank/>) and the pairwise sequence identity values for the nearly complete gene sequences were calculated on EzBioCloud server (<https://www.ezbiocloud.net/>). Phylogenetic analyses for maximum likelihood (ML) and maximum parsimony (MP) methods were conducted by the GGDC web server using the DSMZ phylogenomics pipeline adapted to single genes available at <http://ggdc.dsmz.de/>.

3.3. Nanoparticles Synthesis

For green synthesis of iron oxide nanoparticles, the isolates were grown in TYG broth medium (tryptone 3.0 g/l, yeast extract 5.0 g/l, glucose 5.0 g/l, pH 7) for 12 days at 28°C on a shaker incubator (150 rpm). After incubation, the cultures were centrifuged at 10,000 rpm at 4°C for 10 min and the supernatants were used to synthesize iron oxide nanoparticles. A solution of 5 mM iron (II) chloride tetrahydrate ($\text{FeCl}_2 \cdot 4\text{H}_2\text{O}$) and 10mM iron (III) chloride hexahydrate ($\text{FeCl}_3 \cdot 6\text{H}_2\text{O}$) with ratio (2:1), were prepared in sterilized deionized water and 50 ml of the supernatant was added dropwise with constant stirring. After formation of brown-black precipitates, five drops of NaOH were added to the mixture to stabilize the iron nanoparticles (Figure 3.2) then, the solution was centrifuged to collect the iron nanoparticles followed by washing with sterilized deionized water and ethanol. The iron nanoparticles were dried at 70°C for 2 hours.

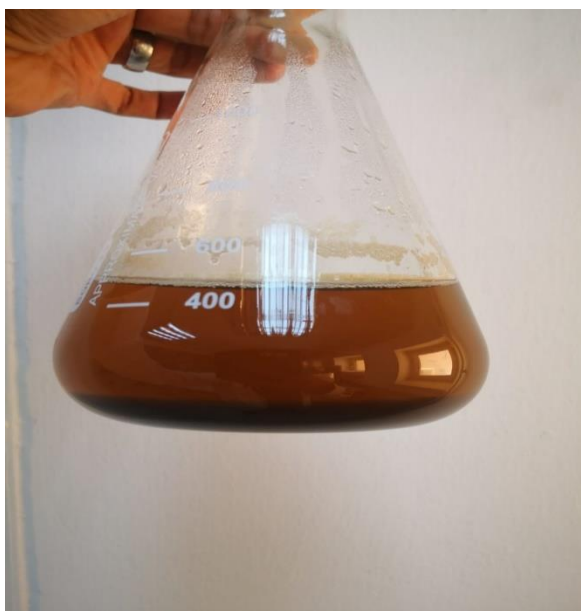


Figure 3.2. Precipitated iron nanoparticles (SP 618)

3.4. Characterizations of Iron Nanoparticles

3.4.1. UV-Vis Spectrophotometry

A UV-visible spectrophotometer (Multiskan Go, Thermo Scientific) was used to characterize the synthesized iron NPs, The UV absorbance of the synthesized iron nanoparticles was measured in the wavelength range of 200-900 nm to confirm the presence of iron nanoparticles.

3.4.2. X-Ray Diffraction (XRD) Analysis

The crystal nature and average crystallite size of the iron oxide nanoparticles was recorded using X-ray diffraction (XRD) (Rigaku) at 40 keV and 30 mA with CuK α radiation (1.5406 Å) in the 2 θ scan range of 5-90°.

3.4.3. Scanning Electron Microscopy (SEM)

The morphological analysis was carried out using a JEOL JMS-7001F scanning electron microscope (SEM) at an accelerating voltage of 15 kV to ascertain the morphology of the iron oxide nanoparticles. A SEM attached EDS equipment is used for the determination of elemental analysis of the nanoparticles.

3.4.4. FT-IR analysis

FTIR examination of the dried powder of produced iron NPs was carried out with a resolution of 4 cm⁻¹ in the range 450–4000 cm⁻¹. These observations were made in KBr pellets using a Perkin-Elmer Spectrum One instrument in diffuse reflectance mode with a resolution of 4 cm⁻¹.

3.5. Heavy Metal Removal Assay

A solution of Pb(II) and Cd(II) (25 ml) was added to 50 ml glass tubes and placed on a shaker. Samples were taken after 120 min under different conditions (solution concentrations of mixed Pb(II) and Cd(II): 30 mgL⁻¹, iron nanoparticle concentrations 0.25, 0.5, 1.0, 1.5 gL⁻¹). The residual concentration of Pb(II) and Cd(II) in the filtrate was measured using an atomic absorption spectrophotometer.

3.6. Dye Removal Activity

Batch adsorption experiments were performed to test the potentiality of the iron-nanoparticles on degradation of Acid Red 337 dye, All dyes adsorption studies were carried out in 50 mL dye-containing solution with a concentration between (0.25 - 2) g L⁻¹ at 25 °C. The 100 mg of iron composites were used at pH to 3 - 6 under vigorous stirring conditions of 150 rpm for 2 h to ensure the extensive adsorption equilibrium. The mixture was separated by centrifugation and collected using filtered liquor to measure dye concentration by UV-Vis technique ("Leaf-nosed bat," 2009). For comparison, each adsorption experiment was conducted twice to depict any adsorption behavior of Acid Red 337 dye by iron-nanoparticles.

Due to the lack of references and experiments to remove this type of dyes using iron nanoparticles, the experiment was conducted on the basis of some experiments with other dyes or other adsorbents (Kamath *et al*, 2019).

The adsorption experiments were performed to evaluate the thermodynamic effects and to obtain adsorption isotherms. Also, studied on the amounts of adsorbed dye ($\text{mg}\cdot\text{g}^{-1}$) were determined from their concentrations, before and after adsorption, by applying Equation:

$$q = \frac{(C_0 - C_e) \cdot V}{m} \quad (3.1)$$

Where C_0 and C_e are the initial and final values of the dye concentration ($\text{mg}\cdot\text{L}^{-1}$), respectively. The volume (L) of the dye solution is represented by V . Furthermore, m is the mass of the adsorbents (g).

Table 3.1. Iron nanoparticles used for dye removal assay

Name	Concentration of nanoparticles	Absorbance of dye	Absorbance after treated by INP	Removal rate %
YS38	0.50 g/l	0.722	0.679	6%
SN43	0.50 g/l	0.722	0.642	11%
SP618	0.50 g/l	0.722	0.602	16.6%
SP654	0.50 g/l	0.722	0.648	10%
SN13	0.50 g/l	0.722	0.673	6%
SN42	0.50 g/l	0.722	0.672	6%

3.6.1. Red Dye Preparation

The pH value of the red acid dye 337 used in the adsorption experiments was adjusted by adding NaOH and HCl solutions. Doses of selected adsorbents were weighed in a micro and applied, Prepared adsorbents were placed in 25 ml bottles in dyes in certain solutions and the final result was compared in an orbital incubator (dye concentration was 50mg/l), After contact, the samples have been centrifuged and the absorption value of the supernatant measured in a DR 5000 UV-Visible spectrophotometer at 500 nm wavelength.

In the previous table, the conditions were fixed pH 3, Time: 2 hours and the best nanoparticles were examined in terms of removal effectiveness is SP618 so we will use it next experiment.

3.6.2. Effect of pH

The values obtained from studies on the effect of changing the pH on the adsorption event, while the highest specific capture value was observed at pH 1, the specific capture amount of the adsorbent dye decreased up to pH with increasing pH, the capture increased, at pH 3. After this value, the increase in pH decreased the capture amount, the trend was horizontal at pH 6, 7 and 8, and there was no excessive increase or decrease in the specific capture.

In adsorption, pH is an important parameter because it affects both surface properties of an adsorbent and the behavior of the adsorbents in solution. This is why there is a necessity to determine the optimum pH value in each adsorption study.

With increasing pH, the negatively charged areas increase on the surface of the adsorbent material, while the positively charged areas decrease. Therefore, the positive charge of the area it will hold allows electrostatic forces to come into play, the negative-charge surface regions on the adsorbents do not favor adsorption of dye ions as a result of the electro-static repulsion. In the adsorption of anionic dyes, if the solution is high, the OH ions compete with the dye anions and the surface of the adsorbent does not favour the adsorption of dye anions (Ozawa *et al*, 2012).

3.6.3. Effect of Contact Time on Adsorption

In order for the adsorption to take place, the adsorbent and the adsorbed substance must come into contact for a certain period of time, Determining the time it takes for the adsorption event to reach equilibrium is important in terms of using the sorbent in practice, The data obtained during the determination of the contact time also gives information about the speed of the process. Thus, kinetic constants are obtained and reactor design data is obtained during the application, It is necessary for performing the test studies in order to accurately determine the kinetic data of adsorption kinetics of the dye in solution (Chang *et al*, 2012).

4. RESULTS AND DISCUSSION

4.1. Identification and Phylogenetic Analysis of *Actinobacteria*

A total of six isolates exhibiting typical actinobacterial morphologies were selected for identification at the genus level. The isolates were determined by the pairwise 16S rRNA gene sequence analyses. For each isolate, an almost full length 16S rRNA gene sequence was acquired and compared with the databases on EzBioCloud and GGDC web servers. Pairwise sequence identity levels of the strains to their closest type species are shown in (Table 4.1). The strains were identified as belonging to the genera *Crossiella*, *Nocardia*, *Saccharothrix*, *Saccharomonospora* and *Streptomyces* (Fig. 4.1 –4.5).

Table 4.1. Pairwise sequence identity levels of strains to the closest type species

Isolate no	GenBank accession number	The closest type strain	16S rRNA gene sequence identity (%)
SN13	OL303922	<i>Nocardia cyriacigeorgica</i> DSM 44484 ^T	100
SN42	OL303923	<i>Crossiella cryophila</i> NRRL B-16238 ^T	98.75
SN43	OL303924	<i>Saccharothrix espanaensis</i> DSM 44229 ^T	99.37
SP618	OL303926	<i>Streptomyces cacaoi</i> subsp. <i>cacaoi</i> NRRL B-1220 ^T	99.79
SP654	OL303929	<i>Streptomyces marokkonensis</i> Ap1 ^T	99.65
YS38	OL303932	<i>Saccharomonospora cyanea</i> NA-134 ^T	98.89

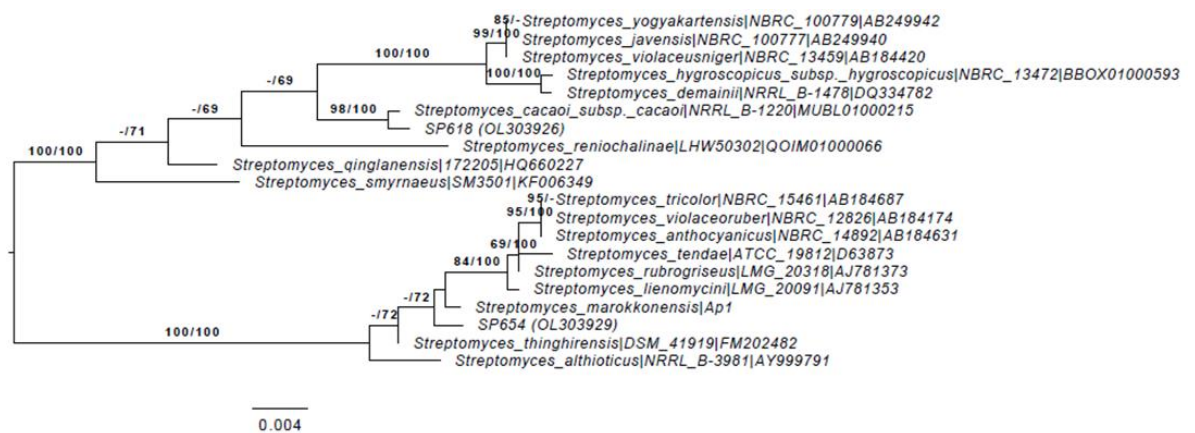


Figure 4.1. Maximum likelihood tree for strains *Streptomyces* spp. SP618, SP654 and its close phylogenetic neighbours interpreted under the GTR+GAMMA model and rooted at the mid-point. Scale bar represents the expected number of the substitutions in each one of the sites. The support values for the bootstrapping have been shown above branches in the case of 60% for the maximal possibility (left) and maximal parsimony (right). GenBank accession numbers for 16S rRNA gene sequences have been provided between the brackets

Strain SP618 is closely related to the type strain of *Streptomyces cacaoi* subsp. *cacaoi* by sharing 99.79% identity level of 16S rRNA gene sequence and it has variation ratio of 3 in 1451 nucleotides. Considering the tree topology, strain SP618 might be a novel species within the genus *Streptomyces*, despite relatively high level of 16S rRNA gene sequence identity. On the other hand, strain SP654 shared 99.65% 16S rRNA gene sequence identity level with its closest phylogenetic neighbour *Streptomyces marokkonensis* with variation ratio of 5 in 1449 nucleotides. However, strain SP654 was well separated from its neighbours in the phylogenetic tree implying its novelty in the genus *Streptomyces*.

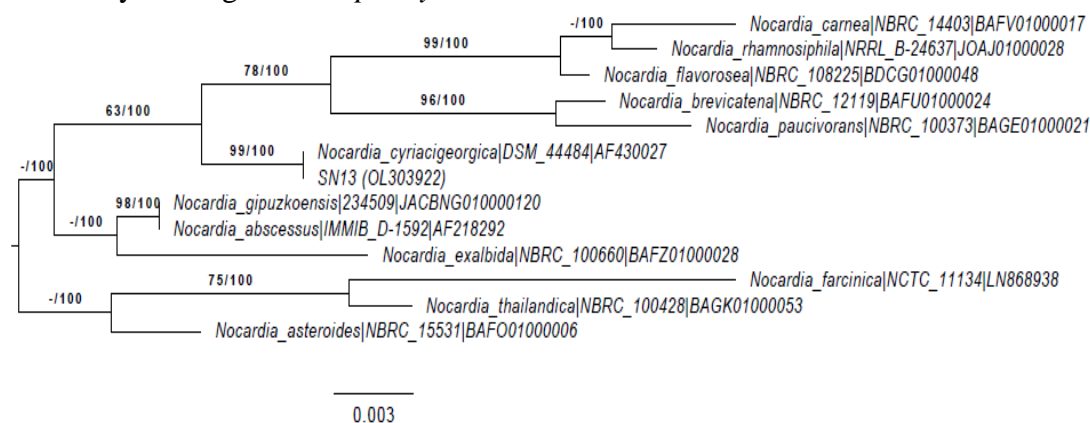


Figure 4.2. Maximum likelihood tree for strain *Nocardia* sp. SN13 and its close phylogenetic neighbours that had been interpreted under GTR+GAMMA model and rooted at the mid-point. Scale bar is indicating expected number of the substitutions in each one of the sites. The support values for the bootstrapping have been illustrated the branches in the case where it is > 60% for the maximal parsimony (right) and maximal possibility (left). GenBank numbers of accession for 16-S rRNA gene sequences have been provided between the brackets (Figure 4.2).

Strain SN13 is found to be member of the genus *Nocardia* and it shares an identical 16S rRNA gene sequence with the type strain of *Nocardia cyriaciageorgica*.

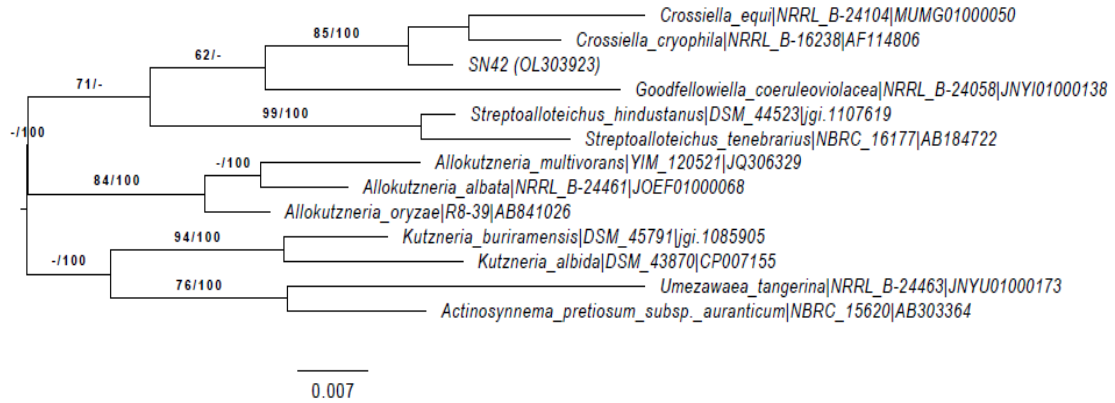


Figure 4.3. Maximum likelihood tree for strain *Crossiella* sp. SN42 and its close phylogenetic neighbours interpreted under GTR+GAMMA model and rooted at the mid-point. Scale bar indicates the expected amount of the substitutions in each one of the sites. Support values for the bootstrapping have been provided above branches in the case where >60% for maximal parsimony (right) and maximal possibility (left). The accession numbers of the GenBank for 16-S rRNA gene sequences have been provided between the brackets

Strain SN42 is found to be a member of a rare actinobacterial genus *Crossiella*. The strain SN42 shares the highest 16S rRNA gene sequence identity level of 98.75% with the type strain of *Crossiella cryophila* with variation ratio of 18 in 1440 nucleotides. Both tree topology and relatively low level of 16S rRNA gene sequence identity level reveal the novelty of strain SN42.

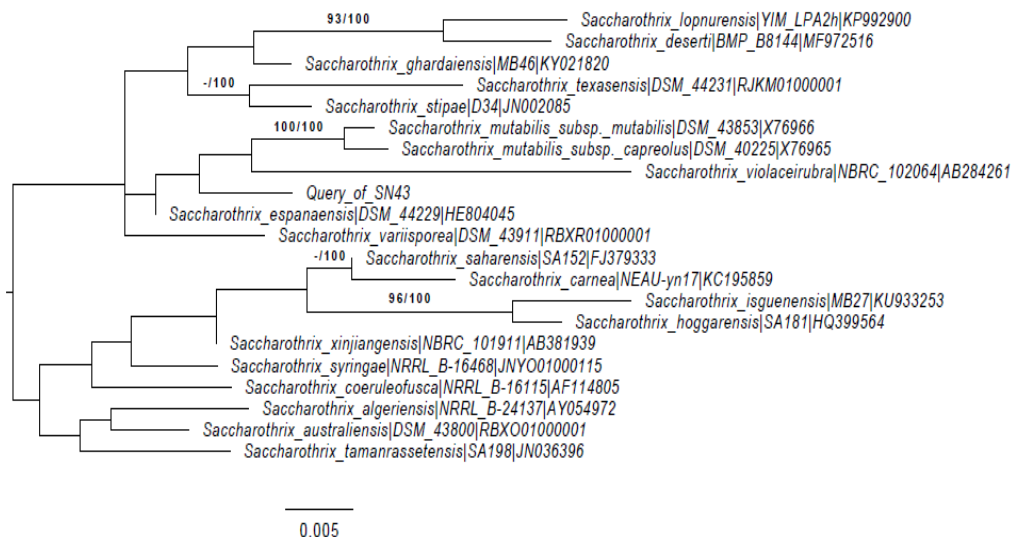


Figure 4.4. Maximum likelihood tree for strain *Saccharothrix* sp. SN43 and its close phylogenetic neighbours interpreted under GTR+GAMMA model and rooted at the mid-point. Scale bar indicates expected amount of the substitutions in each one of the sites. The bootstrapping support values have been given above branches when > 60% for maximal parsimony (right) and maximal possibility (left). The GenBank accession numbers for 16-S rRNA gene sequences have been provided between the brackets

Strain SN43 is closely related to the type strain of *Saccharothrix espanensis* with 99.37% 16S rRNA gene sequence identity level. However, its tree topology shows that strain SN43 represents a novel species within the genus *Saccharothrix*.

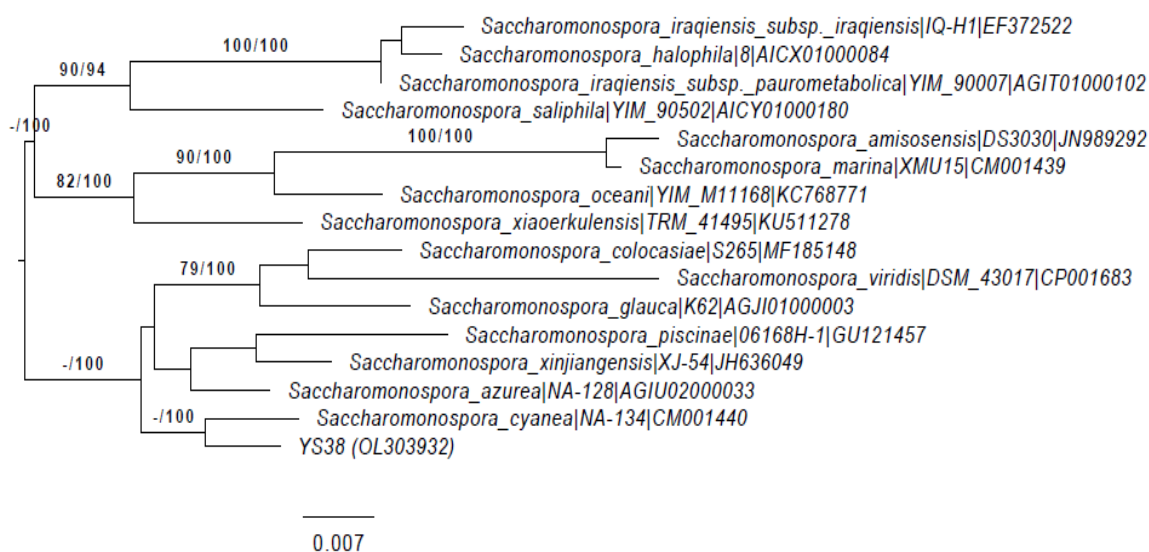


Figure 4.5. Maximum likelihood tree for strain *Saccharomonospora* sp. YS38 and its close phylogenetic neighbours interpreted under the GTR+GAMMA model and rooted at the mid-point. Scale bar indicates expected amount of the substitutions in each one of the sites. The bootstrapping support values are given above branches when > 60% for maximal parsimony (right) and maximal possibility (left). The accession numbers of the GenBank for 16-S rRNA gene sequences have been provided between the brackets

Strain YS38 is closely related to the type strain of *Saccharomonospora cyanea* and it shares 98.89% 16S rRNA gene sequence identity level with variation ratio of 16 in 1445 nucleotides. As can be concluded from the phylogenetic tree, strain YS38 is a representative of a novel species in the genus *Saccharomonospora*.

4.2. Characterization of Iron Nanoparticles Synthesized by *Actinobacteria*

After adding the cell-free broth of each strain to the iron chloride solution, a variation of the color from yellow to brown-black has been observed, which indicated the formation of iron nano-particles. The UV-Vis spectra analysis performed on range of 200-900 nm wavelength showed that the iron nanoparticles synthesized by actinobacteria exhibited the absorption peaks at 250-350 nm ranges as a result of the excitation of surface plasmon vibrations. Further physicochemical characterization based on X-ray diffraction, SEM-EDS and FT-IR analyses was conducted for the nanoparticles synthesized by strain SP618. The XRD pattern of iron nanoparticles that are synthesized by strain SP618 has been shown in (Figure 4.6).

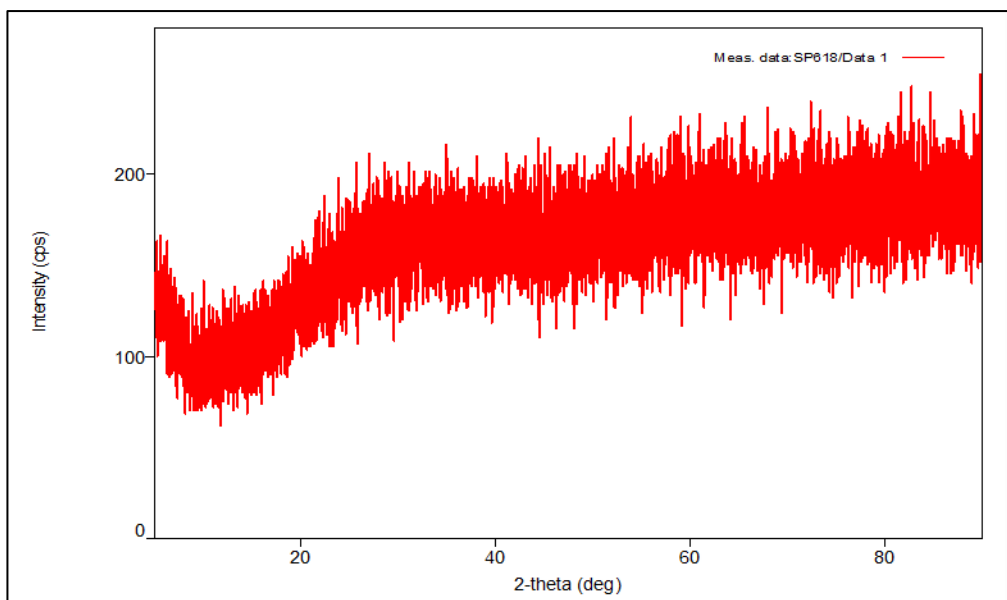


Figure 4.6. XRD patterns of the iron nanoparticles that have been synthesized by strain SP618

The XRD pattern revealed that the nanoparticles had shown deficiency in the distinctive peaks of diffraction that had corresponded to the amorphous nature of those nanoparticles. The NPs morphological characteristics that have been obtained from the strain SP618 have been identified with the use of the SEM (Figure 4.7), the particles that have been amorphous, granular, rough globular surfaced clusters. The synthesized NPs elemental analysis has been performed with the use of the EDX analyses. Energy-dispersive spectrum of the X-ray of iron NPs had affirmed presence of iron region in a range between 2keV and 8keV through the sharp spectral signals (Figure 4.8).

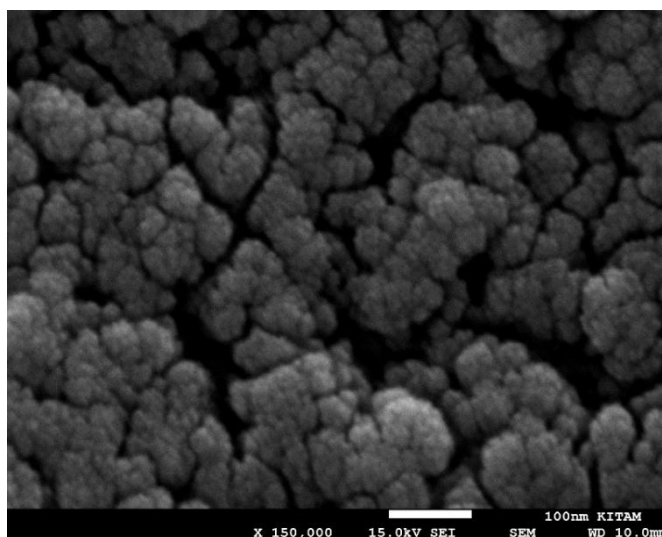


Figure 4.7. SEM image of iron nanoparticles synthesized by strain SP618 at 100 nm scale resolution

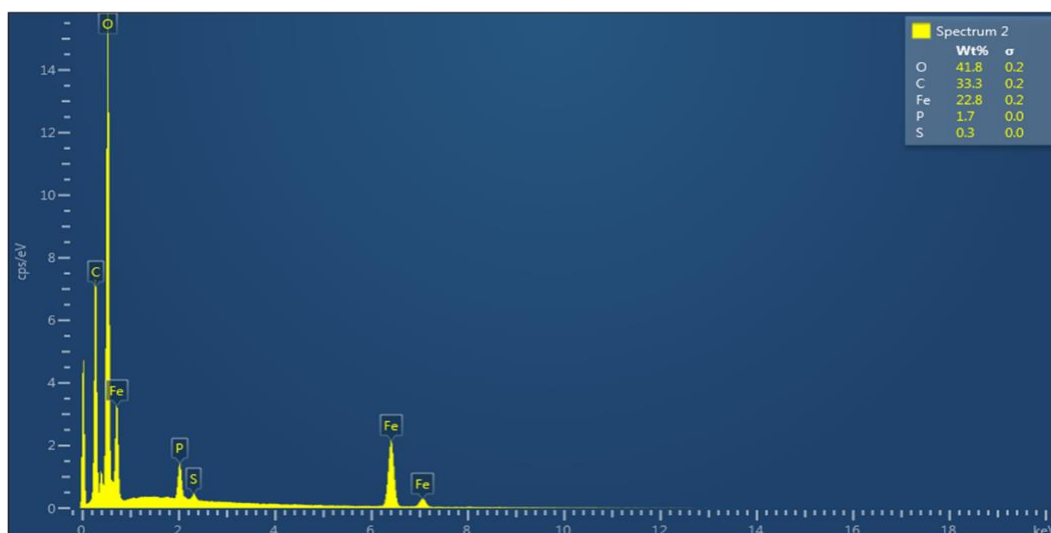


Figure 4.8. EDX results of synthesized NPs possessing strong Iron signals

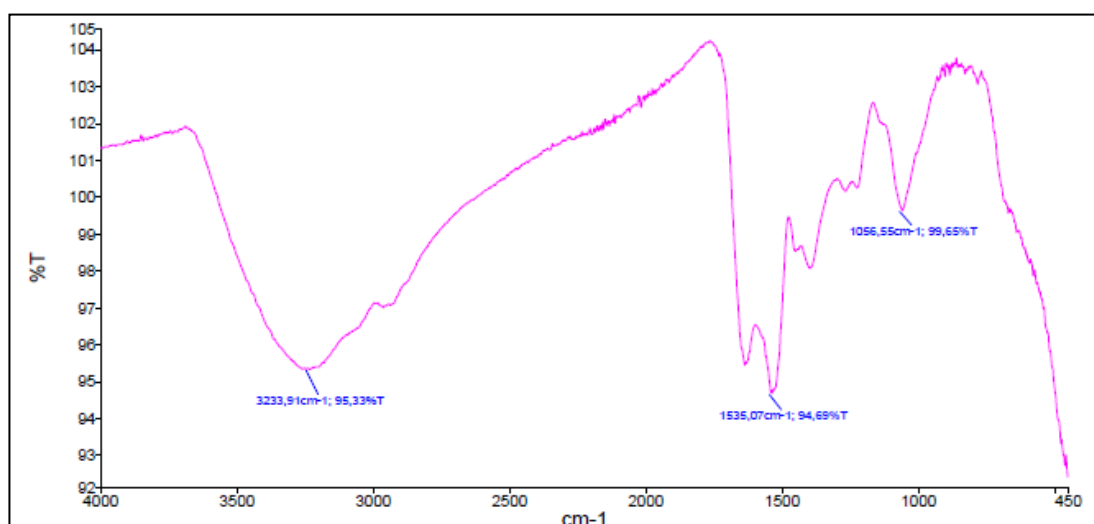


Figure 4.9. FT-IR spectra of iron oxide nanoparticles synthesized by strain SP618

According to the FT-IR analysis, the iron nanoparticles showed strong bands around 1535 cm^{-1} and 3233 cm^{-1} which indicates -OH groups in nanoparticle surface. Another band around 1056 cm^{-1} implies the presence of C-O groups resulting from phenolic compounds produced by the strain SP618.

4.3. Heavy Metal Removal Assay

The iron nanoparticles synthesized by the actinobacteria could not remove lead or cadmium from aqueous solutions (Table 4.2)

Table 4.2.Result of atomic absorption spectroscopy

Pb			
INP		Inaitoal con.	Con. After treating
YS 38		30.68	30.22
SN 43		30.68	30.65
Sp 618		30.68	29.95
SN 42		30.68	30.68
SN 13		30.68	30.61
Cd			
INP			
YS 38		29.35	29.12
SN 43		29.35	29.02
Sp 618		29.35	28.54
SN 42		29.35	29.11
SN 13		29.35	29.22

4.4. Dye Removal Activity

The iron nanoparticles produced by strain SP618 were found to be effective for decolourisation of acid red 337 dye in aqueous solution. The dye solution was treated with the nanoparticles at a range of 1-4 hours at pH 3. After removing the nanoparticles by 0.45 μm filter, the maximum dye removal rate of the iron nanoparticles was calculated as 63% for 4 hours treatment (Table 4.3).

Table 4.3. Different concentration of iron nanoparticles with fix concentration of red dye

Concentration of iron nanoparticles g/l	Co (mg.l)	Ce (mg.l)	Removal rate%
0.25	50	41.51	16.96
0.5	50	40.28	19.42
1	50	31.60	36.93
1.5	50	27.42	45.14

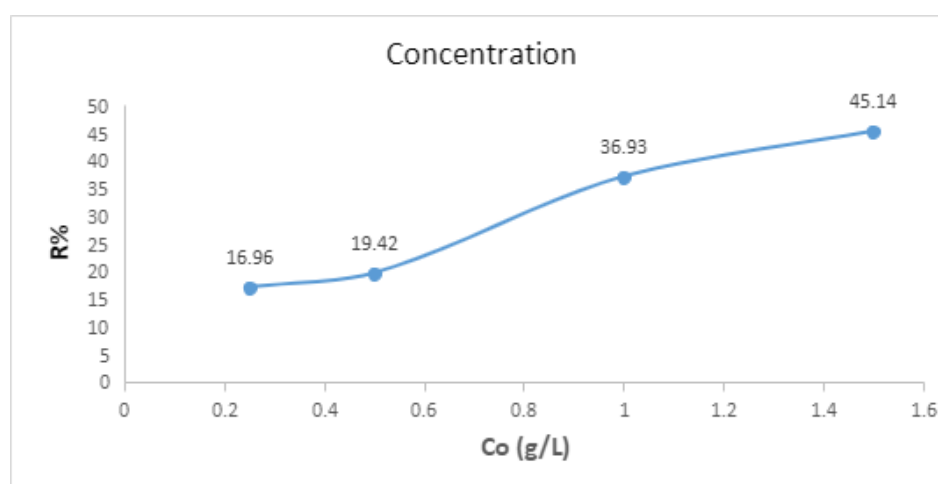


Figure 4.10. Concentration effect

The values obtained from studies on the effect of changing the pH on the adsorption event are shown in (Figure 4.10). while the highest specific capture value was observed at pH 1, the specific capture amount of the absorbent dye decreased up to pH with increasing pH, the capture increased, at pH 3. After this value, the increase in pH decreased the capture amount, the trend was horizontal at pH 6, 7 and 8, and there was no excessive increase or decrease in the specific capture.

In order for the adsorption to take place, the adsorbent and the adsorbed substance must come into contact for a certain period of time. Determining the time it takes for the adsorption event to reach equilibrium is important in terms of using the sorbent in practice. The data obtained during the determination of the contact time also gives information about the speed of the process. Thus, kinetic constants are obtained and reactor design data is obtained during the application. It is necessary for performing the test studies in order to accurately determine the kinetic data of adsorption kinetics of the dye in solution (Rashed, 2013).

Dye concentration was 50 mg/l, nanoparticles concentration was 1.5 g/l , data obtained as a result of kinetic studies are presented in (Table 4.4). As shown in Figurex, the effects of the contact time on adsorption capacity of INPs increases continuously during the first 120 min, and at this point, approximately 57% of the adsorption event is corrected. At the end of 240 minutes, there is not much difference between and 180 min and 240 min.

Table 4.4. Effect of time contact of adsorption

Time	Co (mg.l)	Ce (mg.l)	Removal rate %
1 hours	50	36.488	27 %
2 hours	50	27.503	44 %
3 hours	50	21.262	57 %
4 hours	50	20.781	58 %

After that we tried filter it with 0.45 μm (Djilani, et al., 2015) and the result is shown in (Table 4.5).

Table 4.5. Filter effect with time on adsorption

Time	Co (mg.l)	Ce(mg.l)	Removal rate
1 hours	50	33.92	32%
2 hours	50	25.44	49%
3 hours	50	19.90	60%
4 hours	50	18.53	63%

Three different concentration of dye was checked and the result showed that our iron nanoparticles work better with concentration 50 mg/l (Table 4.6)

Table 4.6. Acid red 337 dye removal activity of iron nanoparticles synthesized by strain SP618

Ci (mg/l)	Ce (mg/l)	R%	Qe (mg/g)
25	9.82	61%	10
50	18.53	63%	21
100	81.17	19%	12

5. CONCLUSIONS

Because of their new physicochemical features as compared to their bulk size components, nanoparticles are often employed to enhance numerous catalytic processes. Nanoparticles are needed in businesses due to their vast range of uses. As previously noted, the physical and chemical techniques of nanoparticle manufacturing have several drawbacks. Because of its environmentally favourable approach, biological synthesis would be a favoured process. However, relatively few research have been published on the variables that influence or are responsible for production of metal NPs. Over the last few decades, microbes have been used to synthesize nanoparticles. It is well known that creation of nano-particles utilizing microbes is a lengthy process when compared to chemical and physical procedures. The use of microorganisms in synthesis is still limited to the lab scale. Efforts have to be made to research the practical applications of microorganisms in the manufacture of NPs. The NPs have previously been utilized in various medicinal applications such as dressing, wound infections, and treatments of the pre-clinical stages. One of the latest researches had shown new exciting biological characteristics of the nano scale which might be translated to new pharmacological and therapeutic treatments.

In the present study, a green synthesis process for iron nanoparticles has been successfully employed using novel actinobacterial strains isolated from soil samples. In phylogenetic perspective, the strains identified in this study have high potential to be novel species within their corresponding genera revealed by the 16S rRNA gene-based analyses. Thus, a comprehensive genome-based analysis is required to ascertain the taxonomic positions of these strains. Moreover, the cell-free broth of strain SP618 was very effective to synthesize amorphous iron oxide nanoparticles. The effectiveness of these nanoparticles on heavy metals removal is too small to be considered effective. However, these nanoparticles have been shown efficient for removal of acid red 337 which is an azo dye utilized commonly in textile industry, and the best condition for removal is at pH 3 with contact time of 4 hours. Therefore, it can be concluded that the iron nanoparticles synthesized by strain SP618 can be used to remove this hazardous recalcitrant dye from aqueous environments.

REFERENCES

- Amkraz, N., Boudyach, E., Boubaker, H., Bouizgarne, B. and Ait Ben Aoumar, A. (2010). Screening for fluorescent pseudomonades, isolated from the rhizosphere of tomato, for antagonistic activity toward *Clavibacter michiganensis* subsp. *michiganensis*. *World Journal of Microbiology and Biotechnology*, 26 (6), 1059-1065.
- Anandan, R., Dharumadurai, D. and Manogaran, G. P. (2016). *Actinobacteria - Basics and Biotechnological Applications . An introduction to actinobacteria*. IntechOpen, 3-36,
- Ay, H. (2021). Genomic insight into a novel actinobacterium, *Actinomadura rubrisoli* sp. nov., reveals high potential for bioactive metabolites. *Antonie van Leeuwenhoek*, 114 (2), 195-208.
- Bhattacharya, D. and Gupta, R. K. (2005). Nanotechnology and potential of microorganisms. *Critical reviews in biotechnology*, 25 (4), 199-204.
- Bhattacharya, S. (2016). Biomimetic Synthesis and Characterization of Water Dispersible Iron Oxide-Graphene Nanocomposites for Medical Applications. Jadavpur University Kolkata, India
- Biswas, A., Bayer, I. S., Biris, A. S., Wang, T., Dervishi, E. and Faupel, F. (2012). Advances in top-down and bottom-up surface nanofabrication: Techniques, applications & future prospects. *Advances in colloid and interface science*, 170 (1-2), 2-27.
- Caputo, F., Vogel, R., Savage, J., Vella, G., Law, A., Della Camera, G., Hannon, G., Peacock, B., Mehn, D. and Ponti, J. (2021). Measuring particle size distribution and mass concentration of nanoplastics and microplastics: addressing some analytical challenges in the sub-micron size range. *Journal of colloid and interface science*, 588, 401-417.
- Castro, L., Blázquez, M. L., González, F. G. and Ballester, A. (2014). Mechanism and applications of metal nanoparticles prepared by bio-mediated process. *Reviews in Advanced Sciences and Engineering*, 3 (3), 199-216.
- Chang, W.-C., Lee, C.-H., Yu, W.-C. and Lin, C.-M. (2012). Optimization of dye adsorption time and film thickness for efficient ZnO dye-sensitized solar cells with high at-rest stability. *Nanoscale research letters*, 7 (1), 1-10.
- Dave, P. N. and Chopda, L. V. (2014). Application of iron oxide nanomaterials for the removal of heavy metals. *Journal of Nanotechnology*, (6), 9-19.
- Dhanasekaran, D. and Jiang, Y. (2016). *Actinobacteria: basics and biotechnological applications*. BoD-Books on Demand 22 - 34,
- Frey, N. A., Peng, S., Cheng, K. and Sun, S. (2009). Magnetic nanoparticles: synthesis, functionalization, and applications in bioimaging and magnetic energy storage. *Chemical Society Reviews*, 38 (9), 2532-2542.
- García-Cañas, V., Simó, C., Castro-Puyana, M. and Cifuentes, A. (2014). Recent advances in the application of capillary electromigration methods for food analysis and Foodomics. *Electrophoresis*, 35 (1), 147-169.

- Ghasemzadeh, G., Momenpour, M., Omidi, F., Hosseini, M. R., Ahani, M. and Barzegari, A. (2014). Applications of nanomaterials in water treatment and environmental remediation. *Frontiers of environmental science & engineering*, 8 (4), 471-482.
- Hodoroaba, V.-D., Rades, S., Salge, T., Mielke, J., Ortel, E. and Schmidt, R. (2016). Characterisation of nanoparticles by means of high-resolution SEM/EDS in transmission mode. IOP Conference Series: Materials Science and Engineering, IOP Publishing, 012006, No.109.
- Ilyas, M., Ahmad, W., Khan, H., Yousaf, S., Yasir, M. and Khan, A. (2019). Environmental and health impacts of industrial wastewater effluents in Pakistan: a review. *Reviews on environmental health*, 34 (2), 171-186.
- Jagessar, R. (2021). Nanotechnology and Nanoparticles in Contemporary Sciences. *Journal of Nanosciences Research & Reports. SRC/JNSRR-119*, 3.
- Järup, L. (2003). Hazards of heavy metal contamination. *British medical bulletin*, 68 (1), 167-182.
- Kamath, S., Ramanjaneyalu, V. G. V. and Kamila, S. (2019). Application of ZnO nano rods for the batch adsorption of Cr (VI): a study of kinetics and isotherms. *Am. J. Applied Sci*, 16 (3), 101-112.
- Karkare, M. (2010). *Nanotechnology: fundamentals and applications*. IK International Pvt Ltd, 10-14,
- Kishor, R., Bharagava, R. N. and Saxena, G. (2018). *Recent Advances in Environmental Management*. CRC Press, 1-25.
- Kouhbanani, M. A. J., Beheshtkhoo, N., Taghizadeh, S., Amani, A. M. and Alimardani, V. (2019). One-step green synthesis and characterization of iron oxide nanoparticles using aqueous leaf extract of *Teucrium polium* and their catalytic application in dye degradation. *Advances in Natural Sciences: Nanoscience and Nanotechnology*, 10 (1), 015007.
- Kyzas, G. Z., Fu, J. and Matis, K. A. (2013). The change from past to future for adsorbent materials in treatment of dyeing wastewaters. *Materials*, 6 (11), 5131-5158.
- Lanzafame, P., Perathoner, S., Centi, G., Gross, S. and Hensen, E. (2017). Grand challenges for catalysis in the Science and Technology Roadmap on Catalysis for Europe: moving ahead for a sustainable future. *Catalysis Science & Technology*, 7 (22), 5182-5194.
- Lapage, S., Shelton, J. E. and Mitchell, T. (1970). *Methods in microbiology*. Elsevier, 1-133.
- Lee, L.-H., Goh, B.-H. and Chan, K.-G. (2020). Actinobacteria: Prolific producers of bioactive metabolites. *Frontiers in microbiology*, 11, 1612.
- Levard, C., Hotze, E. M., Lowry, G. V. and Brown Jr, G. E. (2012). Environmental transformations of silver nanoparticles: impact on stability and toxicity. *Environmental science & technology*, 46 (13), 6900-6914.
- Londoño-Restrepo, S. M., Jeronimo-Cruz, R., Millán-Malo, B. M., Rivera-Muñoz, E. M. and Rodríguez-García, M. E. (2019). Effect of the nano crystal size on

- the X-ray diffraction patterns of biogenic hydroxyapatite from human, bovine, and porcine bones. *Scientific reports*, 9 (1), 1-12.
- Loos, M. (2014). *Carbon nanotube reinforced composites: CNT Polymer Science and Technology*. Elsevier, 30 - 52,
- Maksimović, M. and Omanović-Miklićanin, E. (2017). Green internet of things and green nanotechnology role in realizing smart and sustainable agriculture. VIII international scientific agriculture symposium “Agrosym”, 2290-2295.
- Manivasagan, P., Venkatesan, J., Sivakumar, K. and Kim, S.-K. (2016). Actinobacteria mediated synthesis of nanoparticles and their biological properties: A review. *Critical reviews in microbiology*, 42 (2), 209-221.
- Mardikar, S. P., Doss, V., Jolhe, P., Gaikwad, R. and Barkade, S. (2021). *Handbook of Nanomaterials for Wastewater Treatment*. Elsevier, 867-897.
- Maroufpour, N., Alizadeh, M., Hatami, M. and Lajayer, B. A. (2019). *Microbial Nanobionics*. Springer, 63-85.
- Misk, A. and Franco, C. (2011). Biocontrol of chickpea root rot using endophytic actinobacteria. *BioControl*, 56 (5), 811-822.
- Moerz, S. T., Kraegeloh, A., Chanana, M. and Kraus, T. (2015). Formation mechanism for stable hybrid clusters of proteins and nanoparticles. *ACS nano*, 9 (7), 6696-6705.
- Mohamed, H., Miloud, B., Zohra, F., García-Arenzana, J. M., Veloso, A. and Rodríguez-Couto, S. (2017). Isolation and characterization of actinobacteria from Algerian sahara soils with antimicrobial activities. *International journal of molecular and cellular medicine*, 6 (2), 109.
- Mourdikoudis, S., Pallares, R. M. and Thanh, N. T. (2018). Characterization techniques for nanoparticles: comparison and complementarity upon studying nanoparticle properties. *Nanoscale*, 10 (27), 12871-12934.
- Mueller, N. C. and Nowack, B. (2008). Exposure modeling of engineered nanoparticles in the environment. *Environmental science & technology*, 42 (12), 4447-4453.
- Nath, D. and Banerjee, P. (2013). Green nanotechnology—a new hope for medical biology. *Environmental toxicology and pharmacology*, 36 (3), 997-1014.
- Ozawa, H., Awa, M., Ono, T. and Arakawa, H. 2012. Effects of Dye-Adsorption Solvent on the Performances of the Dye-Sensitized Solar Cells Based on Black Dye. *Chemistry—An Asian Journal*, 7 (1), 156-162.
- Pathak, K., Pattnaik, S. and Porwal, A. (2018). Regulatory Concerns for Nanomaterials in Sunscreen Formulations. *Applied Clinical Research, Clinical Trials and Regulatory Affairs*, 5 (2), 99-111.
- Phu, N., Ngo, D., Hoang, L., Luong, N., Chau, N. and Hai, N. (2011). Crystallization process and magnetic properties of amorphous iron oxide nanoparticles. *Journal of Physics D: Applied Physics*, 44 (34), 345002.
- Rashed, M. N. (2013). Adsorption technique for the removal of organic pollutants from water and wastewater. *Organic pollutants-monitoring, risk and treatment*, 7, 167-194.

- Sajanlal, P. R., Sreeprasad, T. S., Samal, A. K. and Pradeep, T. (2011). Anisotropic nanomaterials: structure, growth, assembly, and functions. *Nano reviews*, 2 (1), 5883.
- Saravanavel, J. (2018). Nanotechnology and Nanogeoscience, Centre for Remote Sensing, Bharathidasan University, No.19.
- Sheikh, M., Rathore, D. S., Gohel, S. and Singh, S. P. (2019). Cultivation and characteristics of the Marine Actinobacteria from the Sea water of Alang, Bhavnagar. 24-68
- Smith, P., Ashmore, M. R., Black, H. I., Burgess, P. J., Evans, C. D., Quine, T. A., Thomson, A. M., Hicks, K. and Orr, H. G. (2013). The role of ecosystems and their management in regulating climate, and soil, water and air quality. *Journal of Applied Ecology*, 50 (4), 812-829.
- Usman, K. A. S., Maina, J. W., Seyedin, S., Conato, M. T., Payawan, L. M., Dumée, L. F. and Razal, J. M. (2020). Downsizing metal–organic frameworks by bottom-up and top-down methods. *NPG Asia Materials*, 12(1), 1-18.
- Ventura, M., Canchaya, C., Tauch, A., Chandra, G., Fitzgerald, G. F., Chater, K. F. and van Sinderen, D. (2007). Genomics of Actinobacteria: tracing the evolutionary history of an ancient phylum. *Microbiology and molecular biology reviews*, 71 (3), 495-548.
- Vijayakumar, R., Murugesan, S. and Panneerselvam, A. (2010). Isolation, characterization and antimicrobial activity of actinobacteria from point calimere coastal region, east coast of India. *Int Res J Pharam*, 1, 358-365.
- Wang, B. (2008). Nanostructured transition metal oxide materials for supercapacitor application, University of Wollongong, Australia, (3)
- Yan, W., Dong, C., Xiang, Y., Jiang, S., Leber, A., Loke, G., Xu, W., Hou, C., Zhou, S. and Chen, M. (2020). Thermally drawn advanced functional fibers: New frontier of flexible electronics. *Materials Today*, 35, 168-194.
- Zhang, T., Lowry, G. V., Capiro, N. L., Chen, J., Chen, W., Chen, Y., Dionysiou, D. D., Elliott, D. W., Ghoshal, S. and Hofmann, T. (2019). In situ remediation of subsurface contamination: opportunities and challenges for nanotechnology and advanced materials. *Environmental Science: Nano*, 6 (5), 1283-1302.
- Zikalala, N., Matshetshe, K., Parani, S. and Oluwafemi, O. S. (2018). Biosynthesis protocols for colloidal metal oxide nanoparticles. *Nano-Structures & Nano-Objects*, 16, 288-299.

APPENDIX

Yeast extract starch agar

Agar	15.0g
Starch	10.0g
Yeast extract	2.0g
Distilled water	1000 ml
PH	7

CZAPEK peptone agar

K ₂ HPO ₃	1.0g
NaNO ₃	3.0g
Sucrose	30.0g
MgSO ₄ *7H ₂ O	0.5g
Yeast extract	20.0g
FeSO ₄ *7H ₂ O	0.01g
KCl	0.5g
Distilled water	1000ml
Agar	15.0g
Peptone	5.0g
PH	7

GYM Streptomyces medium

Malt extract	10.0g
Yeast extract	4.0g
Glucose	4.0g
Distilled water	1000ml
Agar	12.0g
CaCo ₃	2.0g
PH	7

TRYPTONE YEAST EXTRACT AGAR (TYG)

Tryptone	3.0 g
Yeast extract	5.0 g
Glucose	5.0 g
Agar	20 g
Distilled water	1000ml
PH	7

ISP medium 2

Yeast extract	4.0 g
Malt extract	10.0 g
Dextrose	4.0 g
Agar	20.0 g
Distilled water	1000 ml
PH	7

APPENDIX II

APPENDIX II: Solutions Used

1) 20% Glycerol

Prolonged exposure of glycerol suspension, Streptomyces spores or their mycelium at -20°C.
prepared for storage.

- Glycerol (Park, Northampton, UK) 20 ml
- Distilled water 80 ml

Approximately 1.5 ml of 20% v/v glycerol suspension was placed in small screw capped tubes and autoclaved at 121 °C for 15 minutes'

2) Lysozyme (50 mg/ml)

Lysozyme (Sigma) 500mg

TE buffer (10 mM Tris, 1 mM EDTA, pH 8) 10 ml

It was prepared by dissolving 500 mg of lysozyme in 10 ml of TE buffer. 1 ml was divided into 1.5 ml sterile Eppendorf tubes and stored at -20°C until the time of use.

3) TBE Buffer (Tris-Boric acid-EDTA; 10x, pH 8)

Tris 121.10 g

Boric acid (Merck) 61.83 g

EDTA (anhydrous) 5.84 g

ddH₂O 1000 ml

The solution contents were weighed and put into a 1000 ml beaker. 500 ml of DDH₂O was added into it and the solution was kept on a magnetic stirrer until it became clear. The final volume was made up to 1000 ml. +4 by adjusting the pH to 8

Stored at °C.

4) 1xTBE, pH 8

10xTBE buffer 50 ml

ddH₂O 450 ml

It was placed in a 400 ml glass bottle with a cap and kept at room temperature.

5) Bromophenol blue (Loading Buffer)

Bromophenol blue (AppliChem) 40 mg

Glycerol 5 ml

0.5M EDTA 1.5ml

ddH₂O 3.5 ml

After the total volume of 10 ml was prepared, 500 µl was distributed into Eppendorf tubes and stored at +4°C.

APPENDIX III

16S rDNA base sequences of tested organisms

> SN 13

CAGGACGAACGCTGGCGGGCGTGCTTAACACATGCAAGTCGAGCGGTAAGGC
CCTTCGGGGTACACGAGCGGCGAACGGGTGAGTAACACGTGGGTGATCTGC
CTCGCACTCTGGGATAAGCCTGGGAAACTGGGTCTAATACCGGATATGACC
TTACATCGCATGGTGTTTGGTGGAAAGATTTATCGGTGCGAGATGGGCCCGC
GGCCTATCAGCTTGTGGTGGGGTAATGGCCTACCAAGGCGACGACGGGTA
GCCGGCCTGAGAGGGCGACCGGCCACACTGGGACTGAGACACGGCCCAGA
CTCCTACGGGAGGCAGCAGTGGGGAATATTGCACAATGGGCGAAAGCCTGA
TGCAGCGACGCCGCGTGAGGGATGACGGCCTTCGGGTTGTAAACCTCTTTC
GACAGGGACGAAGCGCAAGTGACGGTACCTGTAGAAGAAGCACCGGCCAA
CTACGTGCCAGCAGCCGCGGTAATACGTAGGGTGCGAGCGTTGTCCGGAAT
TACTGGGCGTAAAGAGCTTGTAGGCGGCTTGTGCGGTCGATCGTGAAAAC
TGGGGCTCAACCCCAAGCTTGCGGTCGATACGGGCAGGCTTGAGTACTTCA
GGGGAGACTGGAATTCCTGGTGTAGCGGTGAAATGCGCAGATATCAGGAGG
AACACCGGTGGCGAAGGCGGGTCTCTGGGAAGTAACTGACGCTGAGAAGC
GAAAGCGTGGGTAGCGAACAGGATTAGATACCCTGGTAGTCCACGCCGTAA
ACGGTGGGTACTAGGTGTGGGTTTCCTTCCACGGGATCCGTGCCGTAGCTAA
CGCATTAAGTACCCCGCCTGGGGAGTACGGCCGCAAGGCTAAAACCTCAAAG
GAATTGACGGGGGCCCGCACAAAGCGGCGGAGCATGTGGATTAATTCGATGC
AACGCGAAGAACCTTACCTGGGTTTGACATACACCGGAAACCTGCAGAGAT
GTAGGCCCCCTTGTGGTCCGGTGTACAGGTGGTGCATGGCTGTCGTCAGCTCG
TGTCGTGAGATGTTGGGTAAAGTCCCGCAACGAGCGCAACCCTTATCTTATG
TTGCCAGCGCGTAATGGCGGGGACTCGTGAGAGACTGCCGGGGTCAACTCG
GAGGAAGGTGGGGACGACGTCAAGTCATCATGCCCTTATGTCCAGGGCTT
CACACATGCTACAATGGCCGGTACAGAGGGCTGCGATACCGTGAGGTGGAG
CGAATCCCTTAAAGCCGGTCTCAGTTCGGATCGGGGTCTGCAACTCGACCCC
GTGAAGTTGGAGTCGCTAGTAATCGCAGATCAGCAACGCTGCGGTGAATAC
GTTCCCGGGCCTTGTACACACCGCCCGTCACGTCATGAAAGTCGGTAACACC
CGAAGCCGGTGGCCTAACCCTTGTGGGAGGGAGCCGTCGAAGGTGGGATC
GGCGATTGGGACGAAGTCGTAACAAGGTAGCCGTACC

> SN 42

TCATGGCTCAGGACGAACGCTGGCGGCGTGCTTAACACATGCAAGTCGAGC
GGTAAGGCCCTTCGGGGTACACGAGCGGCGAACGGGTGAGTAACACGTGG
GTAATCTGCCCTGCACTCTGGGATAAGCCTGGGAAACTGGGTCTAATACCG
GATATGACAACTTCTCGCATGGGAGGTTGTGGAAAGTTCCGGCGGTGCAGG
ATGGGCCCGCGGCCTATCAGCTTGTGGTGGGGTAATGGCCTACCAAGGCG
ACGACGGGTAGCCGGCCTGAGAGGGGCGACCGGCCACACTGGGACTGAGAC
ACGGCCCAGACTCCTACGGGAGGCAGCAGTGGGGAATATTGCGCAATGGGC
GAAAGCCTGACGCAGCGACGCCGCGTGAGGGATGACGGCCTTCGGGTTGTA
AACCTCTTTCAGTGCCGACGAAGCGAAAGTGACGGTAGGTACAGAAGAAGC
ACCGGCCAACTACGTGCCAGCAGCCGCGGTAATACGTAGGGTGCGAGCGTT
GTCCGGAATTATTGGGCGTAAAGAGCTCGTAGGCGGTTTGTTCGTCGGCTG
TGAAAACCTCGGGGCTTAACTCTGAGCTTGCAGTCGATACGGGCAGACTTGA
GTTCCGGCAGGGGAGACTGGAATTCCTGGTGTAGCGGTGAAATGCGCAGATA
TCAGGAGGAACACCGGTGGCGAAGGCGGGTCTCTGGGCCGATACTGACGCT
GAGGAGCGAAAGCGTGGGGAGCGAACAGGATTAGATACCCTGGTAGTCCA
CGCCGTAAACGTTGGGCGCTAGGTGTGGGGGTCATTCCACGGCCTCCGTGC
CGCAGCTAACGGATTAAGCGCCCCGCTGGGGAGTACGGCCGCAAGGCTAA
AACTCGAAGGAGTTGACGGGGGCCCGCACAAAGCGGCGGAGCATGTGGATT
AATTCGATGCAACGCGAAGAACCTTACCTGGGCTTGACATACACCGGAAAC
CTGCAGAGATGTAGGCCCCCTTGTGGTTCGGTGTACAGGTGGTGCATGGCTGT
CGTCAGCTCGTGTCGTGAGATGTTGGGTAAAGTCCCGCAACGAGCGCAACC
CTCGTTCATGTTGCCAGCGCGTAATGGCGGGGACTCATGGGAGACTGCCG
GGGTCAACTCGGAGGAAGGTGGGGATGACGTCAAGTCATCATGCCCTTAT
GTCCAGGGCTTCACACATGCTACAATGGCCGGTACAATGGGCTGCTAAGCC
GTGAGGTGGAGCGAATCCCTAAAAGCCGGTCTCAGTTCGGATCGGGGTCTG
CAACTCGACCCCGTGAAGTTGGAGTCGCTAGTAATCGCAGATCAGCAACGC
TGCGGTGAATACGTTCCCGGGCCTTGTACACACCGCCCGTCACGTCACGAA
AGTCGGTAACACCCGAAGCCCATGGCCCAACCCGTAAGGGGGGGAGTGGTC
GAAGGTGGGACTGGCGATTGGGACGAAGTCGTAACAAGGTAGCCGTACCG
GAAGGTGC

> SN 43

TCATGGGCTCAGGACGAACGCTGGCGGGCGTGCTTAACACATGCAAGTCGAGC
GGTAAGGCCCTTCGGGGTACACGAGCGGCGAACGGGTGAGTAACACGTGG
GTAACCTGCCCTGTACTCCGGGATAAGCCTGGGAAACTAGGTCTAATACCG
GATACGACTCCATTGGGCATCTTGTGGGGTGGAAAGTTCCGGCGGTATGGG
ATGGACCCGCGGCCTATCAGCTTGTGGGTGGGGTAGTGGCCTACCAAGGCG
ACGACGGGTAGCCGGCCTGAGAGGGTGACCGGCCACACTGGGACTGAGAC
ACGGCCCAGACTCCTACGGGAGGCAGCAGTGGGGAATATTGCACAATGGGC
GAAAGCCTGATGCAGCGACCCGCGTGAGGGATGACGGCCTTCGGGGTTGTA
AACCTCTTTCAGCAGGGACGAAGCGCAAGTGACGGTACCTGCAGAAGAAGC
ACCGGCTAACTACGTGCCAGCAGCCGCGGTAATACGTAGGGTGCGAGCGTT
GTCCGGAATTATTGGGCGTAAAGAGCTCGTAGGCGGTTTGTTCGTCGGCC
GTGAAAACCTCAGCTTAACGTGGAGCCTGCGGTCGATACGGGCAGACTTG
AGTTCGGCAGGGGAGACTGGAATTCCTGGTGTAGCGGTGAAATGCGCAGAT
ATCAGGAGGAACACCGGTGGCGAAGGCGGGTCTCTGGGCCGATACTGACGC
TGAGGAGCGAAAGCGTGGGGAGCGAACAGGATTAGATACCCTGGTAGTCC
ACGCCGTAAACGGTGGGTGCTAGGTGTGGGGGACTTCCACGTCCTCCGTGC
CGCAGCTAACGCATTAAGCACCCCGCCTGGGGAGTACGGCCGCAAGGCTAA
AACTCAAAGGAATTGACGGGGGCCCGCACAAAGCGGCGGAGCATGTGGATT
AATTCGATGCAACGCGAAGAACCTTACCTGGGCTTGACATGCACCGGAAAC
CTGCAGAGATGTAGGCCTCTTCGGACTGGTGTACAGGTGGTGCATGGCTGTC
GTCAGCTCGTGTGTCGTGAGATGTTGGGTAAAGTCCCGCAACGAGCGCAACCC
TCGTTCCATGTTGCCAGCGCGTAATGGCGGGGACTCATGGGAGACTGCCGG
GGTCAACTCGGAGGAAGGTGGGGATGACGTCAAGTCATCATGCCCTTATG
TCCAGGGCTTCACACATGCTACAATGGCCGGTACAGAGGGCTGCTAAGCCG
TGAGGTGGAGCGAATCCCAAAAAGCCGGTCTCAGTTCGGATCGGGGTCTGC
AACTCGACCCCGTGAAGTCGGAGTCGCTAGTAATCGCAGATCAGCAACGCT
GCGGTGAATACGTTCCCGGGCCTTGTACACACCGCCCGTCACGTCACGAAA
GTCGGTAACACCCGAAGCCCGTGGCCCAACCCGTAAGGGGGGGAGCGGTCTG
AAGGTGGGACTGGCGATTGGGACGAAGTCGTAACAAGGTAGCCGTACCGG
AAGGTGCGGCTGGATCACCTCCTT

> SP 618

CTCAGGACGAACGCTGGCGGCGTGCTTAACACATGCAAGTCGAACGATGAA
CCGGTCTCGGCCGGGGATTAGTGGCGAACGGGTGAGTAACACGTGGGCAAT
CTGCCCTGCACTCTGGGACAAGCCCTGGAAACGGGGTCTAATACCGGATAT
GACCACCGGCCGCATGGTCTGGTGGTGGAAAGCTCCGGCGGTGCAGGATGA
GCCCCGCGGCCTATCAGCTTGTGGTGGGGTGGTGGCCTACCAAGGCGACGA
CGGGTAGCCGGCCTGAGAGGGCGACCGGCCACACTGGGACTGAGACACGG
CCCAGACTCCTACGGGAGGCAGCAGTGGGGAATATTGCACAATGGGCGCAA
GCCTGATGCAGCGACGCCGCGTGAGGGATGACGGCCTTCGGGTTGTAAACC
TCTTTCAGCAGGGAAGAAGCGCAAGTGACGGTACCTGCAGAAGAAGCACCG
GCTAACTACGTGCCAGCAGCCGCGGTAATACGTAGGGTGCAGCGTGTGCC
GGAATTATTGGGCGTAAAGAGCTCGTAGGCGGCCTGTCGCGTCGGATGTGA
AAGCCCGGGGCTTAACCCCGGGTCTGCATTCGATACGGGCAGGCTAGAGTT
CGGCAGGGGAGATTGGAATTCCTGGTGTAGCGGTGAAATGCGCAGATATCA
GGAGGAACACCGGTGGCGAAGGCGGATCTCTGGGCCGATACTGACGCTGAG
GAGCGAAAGCGTGGGGAGCGAACAGGATTAGATACCCTGGTAGTCCACGCC
GTAAACGTTGGGCACTAGGTGTGGGCGGCATTCCACGTCGTCGGTGCCGCA
GCTAACGCATTAAGTGCCCCGCCTGGGGAGTACGGCCGCAAGGCTAAAACT
CAAAGGAATTGACGGGGGCCCGCACAAGCGGCGGAGCATGTGGCTTAATTC
GACGCAACGCGAAGAACCCTTACCAAGGCTTGACATACATCGGAAAACCTCTG
GAGACAGGGTCCCCCTTTGGGTGCGGTGTACAGGTGGTGCATGGCTGTCGTC
AGCTCGTGTCGTGAGATGTTGGGTAAAGTCCCGCAACGAGCGCAACCCTTAT
CCTGTGTTGCCAGCATGCCTTTCGGGGTGGTGGGGACTCACGGGAGACTGC
CGGGGTCAACTCGGAGGAAGGTGGGGACGACGTCAAGTCATCATGCCCTT
ATGTCTTGGGCTGCACACGTGCTACAATGGCCGGTACAATGAGCTGCGATG
CCGTGAGGTGGAGCGAATCTCAAAAAGCCGGTCTCAGTTCGGATTGGGGTC
TGCAACTCGACCCCATGAAGTCGGAGTCGCTAGTAATCGCAGATCAGCATT
GCTGCGGTGAATACGTTCCCGGGCCTTGTACACACCGCCCGTCACGTCACGA
AAGTCGGTAACACCCGAAGCCGGTGGCCCAACCCCTTGTGGGAGGGAATCG
TCGAAGGTGGGACTGGCGATTGGGACGAAGTCGTAACAAGGTAGCCGTACC
GGAAGGTGCGG

> SP 654

GCTCAGGACGAACGCTGGCGGCGTGCTTAACACATGCAAGTCGAACGATGA
ACCACTTCGGTGGGGATTAGTGGCGAACGGGTGAGTAACACGTGGGCAATC
TGCCCTGCACTCTGGGACAAGCCCTGGAAACGGGGTCTAATACCGGATACT
GACCATCACGGGCATCCGTGGTGTTCGAAAGCTCCGGCGGTGCAGGATGAG
CCCGCGGCCTATCAGCTAGTTGGTGAGGTAATGGCTCACCAAGGCGACGAC
GGGTAGCCGGCCTGAGAGGGCGACCGGCCACACTGGGACTGAGACACGGC
CCAGACTCCTACGGGAGGCAGCAGTGGGGAATATTGCACAATGGGCGAAA
GCCTGATGCAGCGACGCCGCGTGAGGGATGACGGCCTTCGGGTTGTAAACC
TCTTTCAGCAGGGAAGAAGCGAAAGTGACGGTACCTGCAGAAGAAGCGCC
GGCTAACTACGTGCCAGCAGCCGCGGTAATACGTAGGGCGCAAGCGTTGTC
CGGAATTATTGGGCGTAAAGAGCTCGTAGGCGGCTTGTACGTCGGTTGTG
AAAGCCCAGGGGCTTAACCCCGGGTCTGCAGTCGATACGGGCAGGCTAGAGT
TCGGTAGGGGAGATCGGAATTCCTGGTGTAGCGGTGAAATGCGCAGATATC
AGGAGGAACACCGGTGGCGAAGGCGGATCTCTGGGCCGATACTGACGCTGA
GGAGCGAAAGCGTGGGGAGCGAACAGGATTAGATACCCTGGTAGTCCACG
CCGTAAACGGTGGGCACTAGGTGTGGGCAACATTCCACGTTGTCCGTGCCG
CAGCTAACGCATTAAGTGCCCCGCCTGGGGAGTACGGCCGCAAGGCTAAAA
CTCAAAGGAATTGACGGGGGCCCGCACAAAGCGGCGGAGCATGTGGCTTAAT
TCGACGCAACGCGAAGAACCTTACCAAGGCTTGACATACACCGGAAAGCAT
CAGAGATGGTGCCCCCCTTGTGGTCGGTGTACAGGTGGTGCATGGCTGTCGT
CAGCTCGTGTCGTGAGATGTTGGGTAAAGTCCCGCAACGAGCGCAACCCTT
GTCCCGTGTTGCCAGCAAGCCCTTCGGGGTGTGGGGACTCACGGGAGACC
GCCGGGGTCAACTCGGAGGAAGGTGGGGACGACGTCAAGTCATCATGCCCC
TTATGTCTTGGGCTGCACACGTGCTACAATGGCCGGTACAATGAGCTGCGAT
ACCGCGAGGTGGAGCGAATCTCAAAAAGCCGGTCTCAGTTCGGATTGGGGT
CTGCAACTCGACCCCATGAAGTCGGAGTCGCTAGTAATCGCAGATCAGCAT
TGCTGCGGTGAATACGTTCCCGGGCCTTGTACACACCGCCCGTCACGTCAG
AAAGTCGGTAACACCCGAAGCCGGTGGCCCAACCCCTTGTGGGAGGGAGCT
GTCGAAGGTGGGACTGGCGATTGGGACGAAGTCGTAACAAGGTAGCCGTAC
CGGAAGGTGCG

> YS 38

CAGGACGAACGCTGGCGGGCGTGCTTAACACATGCAAGTCGAACGCTGAAGC
CCAGCTTGCTGGGTGGAGGAGTGGCGAACGGGTGAGTAACACGTGGGTAAT
CTGCCCTGTACTCTGGGATAAGCCCGGGAAACTGGGTCTAATACCGGATAG
GACATGCTCCCGCATGGGGGTGTGTGGAAAGTTCCGGCGGTACAGGTTGAG
CCCGCGGCCTATCAGCTTGTTGGTGGGGTGATGGCCACCAAGGCGACGAC
GGGTAGCCGGCCTGAGAGGGTGACCGGCCACACTGGGACTGAGACACGGC
CCAGACTCCTACGGGAGGCAGCAGTGGGGAATATTGCACAATGGGCGCAAG
CCTGATGCAGCGACGCCGCGTGGGGGATGACGGCCTTCGGGTTGTAAACCC
CTTTCGCCCCGGGACGAAGCGCAAGTGACGGTACCGGGAGAAGAAGCACCG
GCCAACTACGTGCCAGCAGCCGCGGTAATACGTAGGGTGCAAGCGTTGTCC
GGAATTATTGGGCGTAAAGAGCTCGTAGGCGGTGTGTCACGTCTGCCGTGA
AAACCTGCGGCTTAACCGTGGGCGTGCGGTGGATACGGGCATCACTTGAGT
TCGGTAGGGGAGACTGGAATTCCTGGTGTAGCGGTGGAATGCGCAGATATC
AGGAGGAACACCGGTGGCGAAGGCGGGTCTCTGGGCCGAAACTGACGCTG
AGGAGCGAAAGCGTGGGGAGCGAACAGGATTAGATACCCTGGTAGTCCAC
GCCGTAAACGTTGGGCGCTAGGTGTGGGGCGCTGTTACGTGTCCCGTGCC
GTAGCTAACGCATTAAGCGCCCCGCCTGGGGAGTACGGCCGCAAGGCTAAA
ACTCAAAGGAATTGACGGGGGCCCGCACAAAGCGGCGGAGCATGTGGATTA
ATTCGATGCAACGCGAAGAACCTTACCTGGGCTTGACATGCACCGGATCGC
CTCAGAGATGGGGTTTCCCTTGTGGCTGGTGCACAGGTGGTGCATGGCTGTC
GTCAGCTCGTGTCGTGAGATGTTGGGTAAAGTCCCGCAACGAGCGCAACCC
TTGTCCCATGTTGCCAGCGGGTTATGCCGGGGACTCGTGGGAGACTGCCGG
GGTCAACTCGGAGGAAGGTGGGGATGACGTCAAGTCATCATGCCCTTATG
TCCAGGGCTTCACACATGCTACAATGGCCGGTACAGTGGGTGGCGATACCG
TGAGGTGGAGCGAATCCCTCAAAGCCGGTCTCAGTTCGGATCGCAGTCTGC
AACTCGACTGCGTGAAGTCGGAGTCGCTAGTAATCGCAGATCAGCATTGCT
GCGGTGAATACGTTCCCGGGCCTTGTACACACCGCCCGTCACGTCATGAAA
GTCGGTAACACCCGAAGCCCATGGCCCAACCCCTTGTGGGGAGGGAGTGG
TCGAAGGTGGGACTGGCGATTGGGACGAAGTCGTAACAAGGTAGCCGTACC
G

BACKGROUND

Ali Salih Mohammed was born in Iraq. After graduated from High school, he complete BSc biochemical technology from university of technology in Iraq.

He entered Ondokuz Mayıs University – Nanoscience and Nanotechnology department – Master, program (English) in 2019. Basic interests include reading and travelling.

Education and Qualification

- BSc in biochemical technology from university of technology in Iraq
- Training on T.O.T (training of trainer) from American Canadian board.
- Training on Pharma training program from Drogan Turkish pharmaceuticals company
- Training on Selling skills from JUPHAR drug company
- Training course on analytical measure of hazardous substance in the work environment from (JICA) japan international cooperation agency.

ORCID : 0000-0001-9429-9485

Student number : 18211435

Publications

1. Mohammed, A.S., Akbal, F., Ay, H. (2021). Green synthesis of iron nanoparticles using actinobacteria and their catalytic application in dye removal. 4th International Eurasian Conference on Biological and Chemical Sciences (EurasianBioChem). 24-26 November 2021.